Neuromuscular changes with age: a simulation study

A thesis submitted in fulfilment of the requirements for the degree of

Doctor of Philosophy

Katherine Anne Wheeler

MPhil, B.Eng (Hons), B.Sc

School of Electrical and Computer Engineering,

College of Science, Engineering and Health

RMIT University, Melbourne, Australia.

Submitted March, 2013

DECLARATION BY THE CANDIDATE

(a) except where due acknowledgement has been made, the work is that of the candidate alone (see the Higher Degrees by Research editing policy);

(b) the work has not been submitted previously, in whole or in part, to qualify for any other academic award;

(c) the content of the thesis is the result of work which has been carried out since the official commencement date of the approved research program;

(d) any editorial work, paid or unpaid, carried out by a third party is acknowledged;

(e) ethics procedures and guidelines have been followed.

_____

Katherine Wheeler

DEDICATION

For Alan. Thank you for everything.

ACKNOWLEDGMENTS

Many thanks to my supervisor Prof. Dinesh Kant Kumar, for his guidance and expertise. Thank you for the varied opportunities you gave me and your interest in my work. Also to Prof. Hirokazu Shimada for his mathematical skill, enthusiasm for our work, and for welcoming me to work with him in Japan. I enjoyed our collaboration immensely. Thank you to Prof. Hans Weghorn for giving me the opportunity to study in Germany.

Thanks to Dr Sridhar Arjunan for his advice, collaboration and camaraderie in the laboratory. Thank you also to the other students in the RMIT Biosignals laboratory - I have enjoyed working with you.

I greatly appreciate the support I have had from my friends and family. Thank you for believing in me, accepting the hours I have to work, and for trying to understand what it is I do.

Thank you to my amazingly supportive family; Judy, Ken, Alison, Ben, Jo and Benn, who always believe in me. Also to my grandparents, family-in-law and Alan, who supports me always.

Contents

List of Figures

List of Tables

Summary of work

The neuromuscular system in the human body shows age-associated change from the third decade of life. For people aged 60-75 (the young-old population group), physiological changes are evident, but the effects of these changes such as unsteadiness and falls are far less apparent than in the elderly. Work to quantify muscular changes in the young-old is lacking. Present techniques are inaccurate or invasive - suitable only for small, isolated studies.

In this work, simulation of the surface electromyogram (sEMG) signal is proposed as a method for investigating age-related muscle degeneration. By adapting the model's parameters to reproduce experimental results, the characteristics of ageing muscles can be estimated.

A sEMG/force model capable of simulating signals from human muscles is presented. The model covers four stages of EMG generation; neuronal stimulating pulse, muscle fibre action potential, motor unit action potential and surface EMG simulation. When populated with accurate simulation parameters, it generates both sEMG and force signals that are shown to correlate closely with experimental data.

The model has been implemented and verified against experimental results from two different muscles of the human arm; the biceps brachii and the brachioradialis. Both the sEMG and force outputs are shown to match experimental data recorded from the contracting muscles of human subjects [Wheeler et al., 2010b, Wheeler et al., 2010d, Wheeler et al., 2010a].

The verified model was utilised to study the way in which muscle composition alters with age. Two groups of subjects were studied. The younger group were aged 20-28 years old, while the older group were aged 60-68 years old. Both groups were asked to contract their biceps brachii isometrically at maximum effort while the sEMG and force signals were recorded. Signal features representing the amplitude and spectrum of the sEMG were then calculated.

The sEMG/force model developed for this work was simulated to generate signals representing the muscles of healthy, young adults. Parameter values were taken from distributions based on experimental studies.

Two main parameters are known to vary with age; the number of motor units (nMU) and the ratio of fast to slow muscle fibre types (FFR). The nMU and the FFR are therefore varied to study their impact on the composite sEMG signal. By comparing these simulated signals with the experimental data, the changes to bicep muscle composition with age are quantified. The simulations show that reducing the number of muscle fibres affected the amplitude, while reducing the ratio of fast fibres in the muscle impacts both the median frequency and the amplitude. The simulated data matches experimental results when the number of active motor units is changed from 110 to 65 and the ratio of fast fibres reduced from 0.45 to 0.14.

The work presented in this thesis demonstrates that an accurate sEMG/force model can be used to infer information about physiological variations from the norm. In this work, muscular changes as a result of ageing are quantified using a robust, accurate and non-invasive methodology.

Chapter 1

Introduction

1.1 Neuromuscular changes with age

18.6% of the Australian population is over 60 years of age and this percentage is increasing steadily [ABS, 2009]. A normal part of the ageing process is neuromuscular changes that reduce steadiness and strength. As these changes affect such a large section of the population, it is crucial that the underlying mechanisms behind these neuromuscular changes are understood.

Previous research has focused on the neuromuscular systems of the infirm and elderly, but far fewer studies have investigated changes that occur with young-old subjects aged 60 - 75 years old [Brown et al., 1988].

The following neuromuscular changes are known to occur in the young-old population:

- A loss of muscle mass and muscle force [Williams et al., 2002, Luff, 1998]
- Minimal loss of endurance and fatigue resistance [Moritani et al., 2004, Bazzucchi et al., 2005]

These effects are due to

- A loss of muscle fibres, with preferential atrophy of type II fibres [Evans and Lexell, 1995]
- A reduction in the size of remaining muscle fibres [Doherty, 2001]

Unknown factors in relation to ageing muscles are

- The extent to which senescent atrophy occurs
- How significant the bias towards the reduction in fast fibres is
- Whether these questions can be answered by in-vivo experiments

Current techniques used to measure muscle composition are biopsy or electro-stimulation. Biopsy is invasive [Borg et al., 1987] and electro-stimulation methods are both invasive and imprecise [Mc Comas et al., 1993]. These techniques are therefore unsuitable for population-based studies. To study the effects of aging in the general population, a method is required that allows researchers to investigate the outcomes of senescent atrophy in a non-invasive and reliable manner.

Surface electromyography (sEMG) is the recording of the electrical activity of the muscle from the surface of the skin. It is non-invasive and easy to record, but does not provide detailed information on the muscles as it records the gross signal from all active motor units in the recording field. To overcome this limitation, models for sEMG have been developed. One of the chief uses of modelling is to allow internal process characteristics to be estimated by adapting the model's parameters to reproduce experimental results [Stegeman et al., 2000].

1.2 Neuromuscular models

Currently available models are not capable of accurately simulating the changes in skeletal muscle with age. Models presented by other authors have focused on alternate research di-

rections and have therefore been optimised for those purposes. They are unsuitable to study ageing as they assume single values for input parameters [Kleine et al., 2001], neglect to address the recruitment characteristics of different muscle fibre types [van Veen et al., 1993, Duchene and Hogrel, 2000] or neglect to address the conduction velocity variation between muscle fibre types [Blok et al., 2002]. The majority of models reported also have a single output that represents the sEMG, rather than considering a second output for model verification [Stegeman et al., 2000].

To study muscular changes that take place as a result of ageing, a suitable model must use accurate representations of the parameters known to alter. These include

- Type based muscle fibre conduction velocities
- Type based motor unit firing rates
- Physiologically accurate motor unit recruitment thresholds

In addition, verification against experimental data must be possible. This is achieved through the addition of a second measurable output such as muscle force. To date, no model exists which satisfies all of these requirements.

This thesis reports the development and use of a model focused on the simulation of different motor unit types and thus suitable for identifying age-associated changes to the neuromuscular system. A series of in-vivo muscle experiments are used to first verify the model, then quantify muscle changes with age.

1.3 Research questions

The work reported in this thesis strives to answer the following research questions:

- How does the neuromuscular system change with age?

- Specifically, do different muscle fibre types react the same way to the ageing process?
- Can a sEMG/force model be used to quantify such changes?

1.4 SEMG/force model developed for this work

The sEMG/force model developed for this thesis research is highly versatile and robust. To ensure the model was accurate, the variable muscle parameters were set to values reported in the literature as a result of experimental work. All active motor units (MUs) were considered, rather than a single MU. This is similar to a real muscle, where many motor units fire to achieve contraction.

As the muscle fibre conduction velocities, motor unit firing rates and recruitment thresholds are populated based on motor unit type, this model is suitable for simulating the whole muscle sEMG and muscle force output signals of the biceps of both younger and older subjects.

1.5 SEMG/force model novelty

This sEMG model differs from models presented by previous authors as it strives to closely align the values and distributions of parameters known to change during disease or ageing with those found in-vivo.

This implementation models a lifelike muscle by introducing random elements to give a distribution of parameters, rather than a single value. This distribution of parameter values is seen in real human muscles. Parameters defined by a distribution include the MU size, the firing rate, initial temporal offset and the muscle fibre conduction velocity.

Most significantly, the model is populated with type-based variables for different motor unit types, allowing slow and fast motor units to be simulated and the effects of the decline

in each to be studied. This is particularly important when considering muscle changes with age, as fast fibre MU numbers decline more rapidly than slow fibre MU numbers.

The model includes a type-based motor unit recruitment and firing frequency strategy, in which these parameters have been assigned probabilities based on muscle fibre type, so that type 1 fibres are recruited at low force levels, and type II fibres are recruited with increasing force. Similarly, the firing rate of each motor unit is type based, with firing rates for type I fibres distributed about averages of 8-14 Hz and type II motor units about averages of 12.5 to 24.5 Hz [Gydikov and Kosarov, 1974, Wheeler et al., 2010a].

To ensure that the sEMG model could be accurately validated against experimental data, a second output was added. This model simulates both the sEMG signal and the force output of the skeletal muscle contraction [Wheeler et al., 2010d].

The implementation of the force output is based on the model described by Fuglevand, where each MU is assigned a twitch force [Fuglevand et al., 1993]. The calculated twitch forces are dependent on the recruitment order and the firing rate of each motor unit in the active MU pool. As described above, these parameters are based on the novel distributions in this work. The contraction time of each twitch force is related to its peak amplitude. The total force exerted during a contraction is the summation of the contributing force trains from each active MU.

1.6 Ageing research using the sEMG model

The implemented sEMG/force model was used in conjunction with experiments to study the effects of age on the biceps muscle.

30 subjects participated in the study; 16 aged 20-29 years old and 14 aged 60-69 years old. The subjects performed isometric contractions of the bicep muscle at their maximum voluntary contraction. The average amplitude of the experimental sEMG signals reduced by

53% with age. The mean power frequency reduced by 5.14 Hz.

Simulated sEMG signals were generated to study the effect of changing the number of motor units and the types of motor units present in the muscle. Simulated data was then compared with experimental signals.

Simulations showed that reducing the number of muscle fibres affected the amplitude, while reducing the ratio of fast fibres in the muscle impacted the median frequency and the amplitude. The simulated data matched experimental results when the number of active motor units was changed from 110 to 65 and the ratio of fast fibres reduced from 0.45 to 0.14.

1.7 Organisation of this thesis

Chapter 2 of this thesis outlines the physiological concepts relied upon in this work and includes a review of sEMG and force models. Chapter 3 describes the sEMG/force model developed by the candidate and includes all equations used to generate the signals used in subsequent sections. The parameter values and distributions used to populate the model are listed in Chapter 4. This chapter also describes the processes followed to verify the accuracy of the model and the procedures used to acquire data from experimental subjects.

Chapter 5 focusses on the use of the developed model to study neuromuscular changes with age. A background of ageing studies is provided, along with experimental and simulated results. These results are discussed in Chapter 6. Chapter 7 concludes this thesis, with particular emphasis on responses to the research questions proposed in section 1.3.

Chapter 2

Literature review

2.1 Introduction

This chapter begins by outlining the neuromuscular theory relied upon in this work. A description of the surface electromyogram (sEMG) signal is then given, with explanations as to how this recorded signal is generated. The final sections of this chapter describe sEMG modelling and the current state-of-the-art in the field.

2.2 Neuromuscular theory

The work in this thesis focusses on the surface electromyogram signal, including signal processing methods used for characterisation and modelling techniques to simulate sEMG data. In order to understand the basis of the sEMG signal, this section gives an overview of the underlying neuromuscular processes. The structure of the nerve and muscle systems, the communication channels leading to muscle contraction and a summary of observations regarding human skeletal muscle types are discussed.

2.2.1 Anatomy of the nervous system

The human nervous system is conceptually divided into two parts. The central nervous system (CNS) refers to the brain and spinal cord. The peripheral nervous system contains all the nerves carrying messages to and from the central nervous system and the rest of the body.

Nerves in the peripheral nervous system are either sensory or motor nerves. Sensory (or afferent) nerves transmit information from the periphery of the body to the central nervous system, including temperature, pain and vibration. Motor (or efferent) nerves carry messages from the brain and spinal cord to the periphery, to effect the function of muscles or glands.

2.2.2 Anatomy of the muscle system

There are three kinds of muscles in the body; skeletal, smooth and cardiac. Skeletal muscles are constructed of long, cylindrical cells called muscle cells or muscle fibres. Each muscle fibre is constructed of muscle fibrils (small slender fibres), their sarcoplasm (water-like substance that fills muscle cells, comparable to cytoplasm in other cell types), mitochondria and multiple nuclei, surrounded by the electrically excitable cell membrane (sarcolemma) which receives and conducts stimuli.

The sarcoplasm consists mostly of myofibrils, which are cylindrical bundles of myosin or actin (refer to Figure 2.1). Actin are thin filaments (approximately 7 nm diameter in humans), while myosin are thicker (around 15 nm) and shaped with head and tail areas [Cooper, 2000]. It is the movement of actin and myosin relative to one another which results in muscle contraction. Each myofibril is composed of many short units, laid end to end, called sarcomeres. Sarcomeres represent the minimal contractile unit of the muscle and it is the contraction of millions of these units that gives rise to muscle activity. The sarcomere can not actively expand, it can only be stretched back to its non-contractive state. Thus, skeletal muscles appear in opposing pairs, so that contraction of one muscle results in the passive stretching of the opposing muscle.

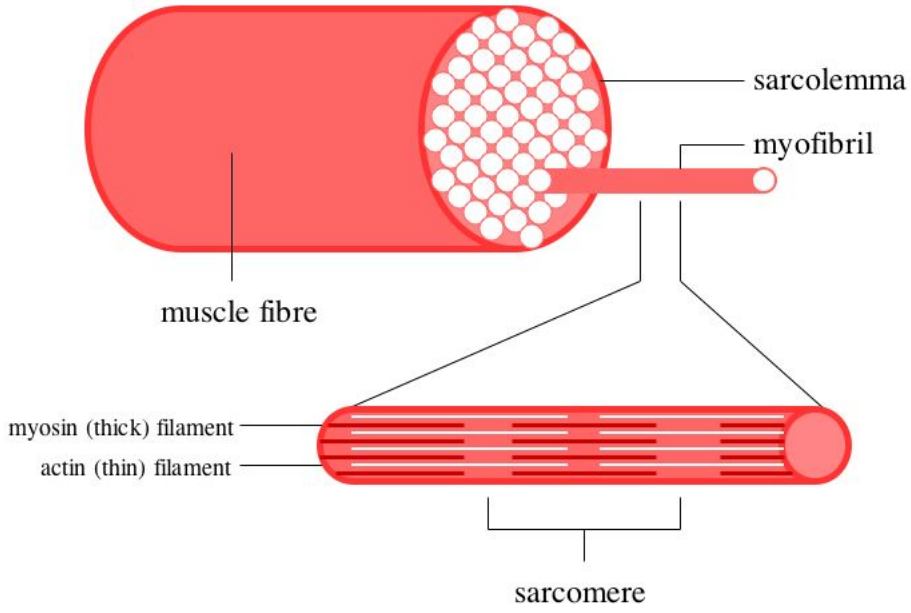

Figure 2.1: Structure of a muscle fibre

The muscle fibres are arranged in groups called motor units. A single motor unit is defined as a motor neuron and the muscle fibres associated with that neuron. The fibres of a motor unit are not always physically adjacent to one another, but are found throughout the muscle volume.

2.2.3 The neuromuscular junction

The neural action potential (AP) is the main method of communication in the nervous system. It is an electrochemical message which is transferred along the nerve fibre as an ionic current between the intracellular and extracellular spaces. Action potentials are electrical signals that obey the "all or nothing" law; i.e. when an axon is electrically stimulated, it will only be activated at a given threshold intensity.

The motor neurons terminate in structures called motor end-plates or neuromuscular

junctions. When an AP travelling down a motor neuron arrives at the neuromuscular junction, ion channels in the muscle cell open, allowing sodium ions to flow in and potassium ions to flow out of the muscle cell's sarcoplasm. The sodium/potassium channels across which the ions flow are more permeable to sodium than potassium, so a greater number of sodium ions flow into the cell than the potassium ions that flow out.

This results in a local depolarisation of the motor end plate, known as an end plate potential (EPP). The action potential causes the sarcoplasmic reticulum to release calcium ions into the sarcoplasm of the muscle fibre [Martini, 2004, Kandell et al., 2000].

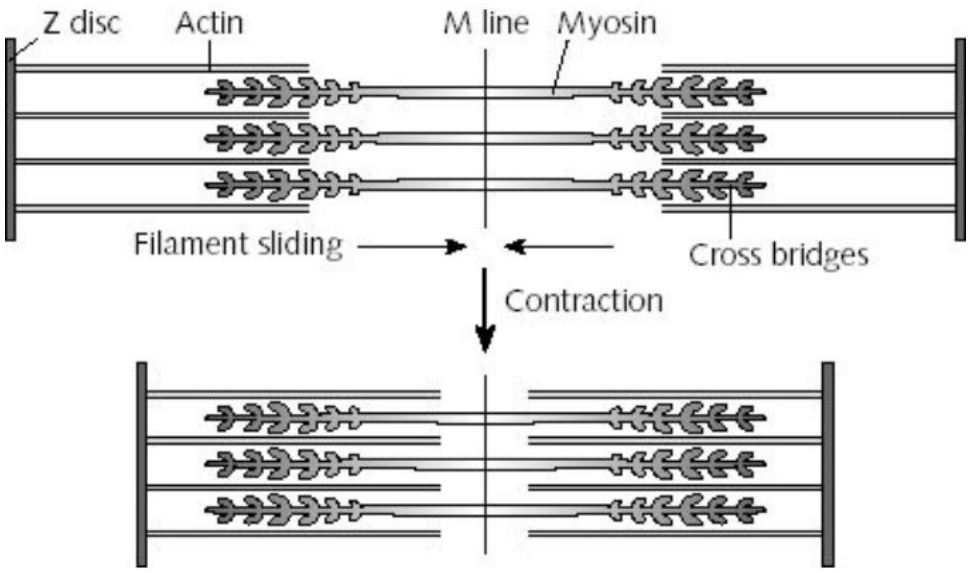

Figure 2.2: Contractions resulting from actin and myosin fibres sliding across each other [Jennett, 1989]

2.2.4 Biomechanics of muscle contraction

Following an end plate potential, the presence of both calcium ions ($Ca2^{+}$) and adenosine triphosphate (ATP) allow contraction of the muscle cell to occur. Calcium ions draw away

the protein which covers actin in its resting state, exposing the actin binding sites. With these sites exposed, myosin binds with the actin, hydrolysing ATP to use as the energy source to bend the myosin heads. The bending of these heads pulls the actin across the myosin in a sliding motion, resulting in a muscle contraction [Cooper, 2000]. This action is shown in Figure 2.2.

After contraction, the calcium ions are returned to the sarcoplasmic reticulum to prepare the muscle cell for its next contraction. This is done through a combination of pumping across the cell membrane and active transportation.

2.2.5 Control of skeletal muscle activity

As in the nervous system, muscular activity is gained by muscule action potentials, described in section 2.2.3. When a neural AP is detected at the neuromuscular junction, it generates a muscular AP in every muscle fibre in that motor unit. Force in skeletal muscles is modulated by either the recruitment of additional motor units, or by increasing the firing frequency of active motor units.

2.2.6 Skeletal muscle fibre types

Skeletal muscle fibres vary in size, diameter and conduction velocity. Although these properties vary on a continuum, there are generally agreed to be three clusters of properties which are identified as the three types of skeletal muscle cells; fast fibres, slow fibres and intermediate fibres.

- Fast fibres

  The majority of muscle fibres in the human body are fast fibres (or type IIb muscle fibres). They contract rapidly (<0.01 seconds) and also fatigue rapidly. Fast fibres are large in diameter and contain densely packed myofibrils, resulting in powerful contrac-

tions. In comparison to slow muscle fibres, fast fibres have a faster rate of depolarisation and repolarisation, a shorter duration action potential, and a lower resting potential [Moritani et al., 2004].

- Slow fibres

  Slow muscle fibres (type I) are smaller in diameter and take about 3 times longer than fast fibres to contract. They are capable of contraction over extended periods, as they do not fatigue as quickly as fast fibres. This is largely due to increased oxygen supply which allows contraction to continue.

- Intermediate fibres

  Intermediate fibres (type IIa) are between fast and slow muscle fibres and have a correspondingly medium size and contraction speed. In muscles containing a mixture of intermediate and fast fibres, physical conditioning can affect the fibre composition.

Motor unit property	**Type I**	**Type IIa**	**Type IIb**
Name	Slow twitch (S or SO)	Fast twitch (FR or FOG)	Fast twitch (FF or FG)
Fatigue resistance	Fatigue restistant	Fatige resistant	Fatigable
Fibre diameter	Small	Intermediate	Large
Conduction velocity	Low	Intermediate	Fast
Recruitment order	Recruited at low force levels	Recruited at intermediate force levels	Recruited at high force levels
Metabolic properties	Oxidative, require adequate oxygen and blood flow	Oxydative, glycolytic	Glycolytic, work well in low oxygen or blood flow conditions

Table 2.1: The physiological properties of muscle fibres. It should be noted that these properties are generalisations; in some cases, such as back muscles, type II fibres do not have larger diameters than type I.

Antigravity muscles (e.g. the back muscles used for posture maintenance) tend to be made up of mostly type I fibres. Muscles which contract for rapid movement contain a similar proportion of type I and type II fibres. Some muscles, such as those in the human hand, contain no slow fibres, as they are used exclusively for brief, rapid contractions. Specific parameters of each muscle type are shown in Table 2.1.

The three types of muscle fibres appear to be randomly distributed across the cross section of the muscle [Moritani et al., 2004], meaning that the study of a particular muscle fibre type is generally possible only with needle electrodes.

2.2.7 Musculature of the human arm

Four muscles of the human arm contribute to flexion of the elbow; the brachialis, the brachioradialis and the two heads of the biceps brachii. In this work, the brachioradialis and the biceps brachii are studied. This section summarises the functionality of each of these muscles.

2.2.7.1 Biceps brachii

The biceps brachii is a large muscle in the upper arm. Its functions include:

- Flexion of the elbow
- Supination of the forearm (turning the palm upwards)
- Abduction of the arm when it is laterally rotated
- Adduction of the arm when when it is medially rotated
- Stabilisation of the shoulder joint when the arm is carrying a heavy load

The biceps brachii is innervated by the musculocutaneous nerve from fibres of the fifth and sixth cervical nerves [Gray, 1973].

2.2.7.2 Brachioradialis

The brachioradialis is a muscle in the human forearm. When the forearm is rotated half-way between pronation and supination, the brachioradialis flexes the forearm. It does not generate as much force as the biceps, as the insertion point is far from the fulcrum of the elbow. The brachioradialis also stabilises the elbow when it is in mid-flexion [Bowden and Bowden, 2002].

The brachioradialis is innervated by the radial nerve.

2.2.8 Skeletal muscle contraction types

There are three types of muscle contraction; isometric, isotonic and isokinetic. Isometric contraction is when the muscle length remains constant, but the tension increases. This is achieved by keeping the limb stationary, while doing work with the muscle of interest. Isotonic contraction is when the muscle length shortens while the tension remains approximately the same. Isokinetic contraction is when the speed of movement is fixed, and the resistance varies with the force required.

To study the neuromuscular system, most experimentalists employ isometric contractions. Isometric contractions have a number of advantages of isotonic or isokinetic movements. Namely

- A significantly lower chance of movement artefact in the recorded signal
- An easily controllable experimental protocol
- The availability of vastly more experimental data for comparison
- The muscles do not shorten, so the innervation zone moves very little

Isometric contractions are therefore used for the work described in this thesis. To investigate the muscle activity present during the muscle contractions, an electromyogram is used.

2.3 The electromyogram

An electromyogram (EMG) measures the voltage gradients produced by contracting muscle fibres. As with neural cells, a muscle cell has a resting membrane potential of around -70 mV, which represents a negative charge inside the cell with respect to the extracellular charge. When a muscle cell contracts, the membrane potential becomes more positive as the sodium ions enter the cell. An electromagnetic field is generated around the muscle fibres by a combination of the membrane depolarisation and the movement of ions. A recording electrode placed in this electromagnetic field will detect the potential difference, or voltage with respect to ground. It is this voltage which is represented by the EMG signal.

The EMG is a differential signal that can be recorded by needle electrodes injected into a muscle (needle EMG), by electrodes injected into the extracellular space in the muscle body (intra-muscular EMG), or by surface electrodes placed on the surface of the skin (surface EMG). In the latter two cases, the recorded EMG is the summation of the action potentials of many muscle fibres [Loeb and Gans, 1986] [Basmajian, 1978]. In experimental conditions, this signal, the algebraic sum of all local action potentials, is often referred to as the Compound Muscle Action Potential (CMAP).

When two recording electrodes are positioned parallel to the muscle fibres, the recorded action potentials will be triphasic in shape, with a polarity that is dependent on the direction from which the action potentials approach the electrode site [Basmajian, 1978].

EMG exhibits the fractal property of self-similarity. This is because the measured EMG signal is created by action potential sources over a range of scales, originating from different locations in the muscles [Arjunan and Kumar, 2007]. Each signal source (motor neuron) has its own recruiting level and discharge threshold, resulting in a complex, non-linear, non-stationary signal.

2.3.1 Uses of the electromyogram

EMGs are recorded from humans in a diagnostic capacity, as changes in the size, shape and frequency of the signal can indicate a myriad of medical conditions including nerve lesions, dermatomyositis and motor neurone disease.

The EMG signal from muscle contraction in an amputated limb is used to control certain types of prostheses. Current technology uses EMG signals for simple movements such as open/close of the prosthetic hand [Zecca et al., 2002], but advances in sEMG signal processing and electrode array manufacture are sure to see this capability improve [Tenore, 2007].

The field of electromyography is vital and extensive, as researchers seek to use the muscular electrical signals to

- Study the neuromuscular system, particularly in regards to ageing, disease and injury
- Advance the control of prosthetic limbs
- Diagnose neuromuscular diseases
- Improve sports medicine techniques and assist athletes with gait, training and recovery

As sEMG signals are a result of muscle activity, certain signal features have a relationship with muscle composition, contraction type, fatigue state and muscle force.

2.3.2 Electromyogram with muscle force

The force exerted by a given muscle is determined by the fibre type composition, the number of active motor units, and the firing frequency of these motor units. The more motor units that are active, and the greater their firing frequency, the greater the muscle force will be.

As a general rule, with increasing force, more motor units are recruited. When a maximal number are active, the firing rate of these motor units rises to further increase the force.

In the hands, where the muscle fibres are all type I, motor unit recruitment is essentially complete at 50% of the voluntary contraction strength. Beyond this point, increases in the firing frequency (also called rate coding) modulate the force. In muscles comprising types I and II fibres, such as the biceps, motor unit recruitment may continue to increase until the force is more than 80%MVC [Moritani et al., 2004] [Kukulka and Clamann, 1981].

The number of active motor units and the rate coding of these units determine the electrical activity of the muscles. Thus, there is a direct relationship between a measured electromyogram and the muscle force output.

2.4 Surface electromyogram models

A recorded sEMG signal depends upon a large number of physiological and anatomical parameters. To increase the understanding of the sEMG signal and what it represents, it is necessary to understand these parameters and the ways in which they influence the signal. Modelling is one method by which this understanding can be improved.

The modelling of biological systems allows the manipulation of variables not possible in vivo. Physical processes can be studied by adapting the model's parameters to generate signals which reproduce those found experimentally [Stegeman et al., 2000].

A model can simulate real world systems in one of three ways; descriptively, phenomenologically, or structurally. In the work described here, a structural model is used, which represents the main elements of the real-life system. To model the individual motor-unit action potentials (MUAPs), precise descriptions of MU anatomy are used.

For a comprehensive description of the variables considered and implemented in the model used in this thesis, refer to Chapter 3. This section gives an overview of the field of surface electromyogram modelling.

The most basic muscle movement is a static contraction; an isometric contraction of

constant force. In this case, in the earliest sEMG models, the contraction was simulated as the sum of a number of MUAPs. Such models were presented by DeLuca [DeLuca, 1975] [DeLuca, 1975], Pan [Pan et al., 1989] and Christakos [Christakos, 1982], among others.

In the mid 1990s, a number of phenomenological models were described, which used autoregressive models to generate sEMG signals. These models simulated accurate signals, but as they were not based on the structure of the muscular system, physiological parameters could not be altered [Merletti and Lo Conte, 1995, Lo Conte and Merletti, 1995].

More recently, structure based models have been developed to allow the physiological properties of individual motor units to be incorporated. As each of these models has been designed to study a certain aspect of either the sEMG signal or the neuromuscular system, the assumptions made are varied.

Fuglevand reported the now commonly used Henneman's size principal, where progressively larger motor units become active with increasing muscle force [Fuglevand et al., 1993]. While certainly more accurate, particularly for isometric muscle contractions, the relationship between recruitment threshold and MU firing frequency remains oversimplified when compared to experimental results [Gydikov and Kosarov, 1974].

The relationship between the voltage and current distributions in an active muscle cell were defined in the important work by Van Veen [van Veen et al., 1993]. This relationship is used by many researchers, including this author, to generate the single fibre action potential current distribution. As the model used in Fuglevand's work was focussed on the intra and extra-cellular muscle fibre currents, it did not consider the differences in recruitment characteristics between slow and fast motor unit types. Similarly, the detailed model reported by Duchene, which focused on simulation efficiency and variable electrode configurations, did not include consideration of type I and II motor units [Duchene and Hogrel, 2000]. Arabadzheiv outlined a model that took into consideration different muscle fibre types when studying synchronisation. This moved his model closer to a physiologically accurate representation

[Arabadzheiv et al., 2010].

Klein and his colleagues implemented an sEMG model to studying the effect of motor unit synchronisation [Kleine et al., 2001]. The model simulated a pool of active motor units with a Gaussian distribution of input voltages (i.e. activation thresholds). A novel synchronisation paradigm was used to simulate the effect on the whole muscle sEMG of motor units firing at the same time. However, model parameters including conduction velocity, MU size and muscle fibre length were assigned single values across the entire MU population, limiting the physiological accuracy of the simulated signals.

Following this work, Blok reported an sEMG model to study the effects of volume conduction on the sEMG signal [Blok et al., 2002]. The model supported the inclusion of multiple tissue layers, tissue anisotropy and consideration of the boundary conditions between layers. However, due to the focus of the work, the model itself was simplified. Concessions included a single value for muscle fibre conduction velocity and the investigation of only a single motor unit action potential.

The work of many key authors has included models which have a single output that represents the sEMG signal [Stegeman et al., 2000, Stegeman et al., 2004, Wakeling, 2009]. In order to ensure that the models are not self-validating, a second output should be considered. The work of Fuglevand and his colleagues defined a method of simulating the force signal from a pool of active motor units [Fuglevand et al., 1993]. This method is described in detail in section 4.2.4. Although the model includes a highly detailed force output calculation, the neural input was simplified to require few parameters. The recruitment thresholds were based on an exponential relationship, where many neurons had low thresholds, and relatively few were assigned high thresholds. The firing frequencies of each motor unit were not related to either the recruitment threshold, or the motor unit type.

Finally, Merletti and Farina have reported a number of models that study aspects of sEMG signal generation. The seminal work by Merletti in 1999 modified the work of Rosenfalck

and Van Veen to provide an intricate and versatile sEMG model [Merletti et al., 1999a]. Farina has used this model to investigate electrode size and shape [Farina et al., 2002a, Mesin et al., 2009], varying conduction velocity [Farina et al., 2002b], properties of volume conduction [Farina et al., 2004] and pinnation [Mesin et al., 2011]. More recent work has sought to study MU signals by decomposition of the sEMG signal [Merletti et al., 2008, Farina and Enoka, 2011]

2.5 Surface electromyogram model to study ageing

As described in section 1.2, a model to study muscular changes that take place as a result of ageing must use accurate representations of the parameters known to alter. These include

- Type based muscle fibre conduction velocities
- Type based motor unit firing rates
- Physiologically accurate motor unit recruitment thresholds

In addition, verification against experimental data must be possible. It is proposed that a model that simulates two outputs rather than a single output allows stronger verification of the strength of the model. For example, if a model simulates both electrical (sEMG) and mechanical (force) outputs, these can both be tested against experimental data to evaluate the accuracy of the chosen input parameters and the model architecture.

Table 2.2 summarises the suitability of the models reviewed in this chapter to investigate muscular changes with age. It is clear that to date, no model exists which satisfies all of these requirements. To study how muscle composition in the young-old differs from that of young, healthy adults, such a model is required. The work in this thesis therefore includes the implementation of a suitable sEMG model, the validation of said model against experimental results, and the utilisation of the model to study muscular changes in the biceps brachii with age.

Model	Type based CV	Type based firing rates	Accurate recruitment paradigm	Second output for validation
Fuglevand 1993	No	No	Yes	No
Van Veen 1993	No	No	Yes	No
Duchene 2000	No	No	No	No
Klein 2001	No	No	No	No
Blok 2002	No	No	No	No
Fuglevand 1993	No	Yes	No	Yes
Merletti 1999	Yes	Yes	Yes	No

Table 2.2: State of the art sEMG models assessed against the key muscular characteristics to alter with age

Chapter 3

Time invariant whole muscle surface EMG/force model

3.1 Introduction

This chapter describes the whole muscle sEMG/force model implemented for this thesis. The model simulates the surface electromyogram signal and the mechanical force generated by a contracting skeletal muscle. The model is physiologically accurate; populated by parameter values from experimental results. The model simulates the neural input signal, the subsequent contraction of muscle fibres, and the effect of volume conduction on the signal detected at the surface of the skin.

Early parts of this chapter describe the neural input signal, the muscle fibre action potential and the generation of motor unit signals. These equations and theories follow the work of Rosenfalck [Rosenfalck, 1969] and Merletti [Merletti et al., 1999a, Merletti et al., 1999b]. The novelty of this model is described in subsequent sections, where the addition of force as a second output, the implementation of a novel firing frequency and motor unit recruitment strategy and the consideration of motor unit types is described.

3.2 Neural action potential

In the human body, voluntary muscle contraction is controlled by the brain. Signals from the brain travel via motor neurons to peripheral skeletal muscles. At the neuromuscular junction, these signals pass from the nervous system to the muscular system.

As with the human body, the input to the model is the action potential signal from the motor nerve. This signal can be modelled by an impulse function ([DeLuca, 1975] with the equation

$$\delta(t - (n \times IP) - \tau_m) \tag{3.1}$$

This is a time domain signal which repeats at a rate of 1/r, where r is the duration between subsequent impulses (in ms). As the firing rate is not constant in-vivo, the value of r in the model changes after each pulse, such that the interpulse duration (IP) is given by

$$IP = r + \delta r \tag{3.2}$$

τ_m is an initial temporal offset. The value of τ_m is different for each motor unit and is assigned randomly. This ensures that each motor unit begins firing at a different time with respect to the remaining active motor units. This scenario mimics that found in the body, where motor units fire randomly with respect to one another to ensure smooth movement. If all motor units started firing simultaneously, the muscle would spasm. The addition of τ_m to the neural pulse train ensures that this does not occur.

The impulse function that simulates the neural action potential train is shown in Figure 3.1.

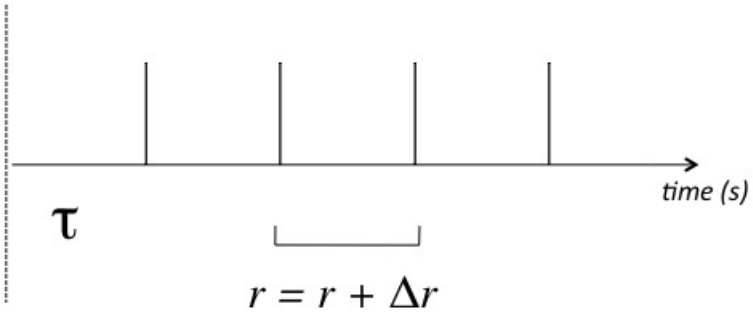

Figure 3.1: The neural input is simulated as an impulse function with a slight variance (jitter) between subsequent pulses

3.3 Voltage distribution of a muscle fibre action potential

When an action potential from the motor neuron arrives at the neuromuscular junction (NMJ), it elicits two muscle action potentials in all the muscle fibres it innervates (i.e. all the muscle fibres in the motor unit). These action potentials (APs) travel from the NMJ towards the tendons at each end of the muscle, where the signals terminate.

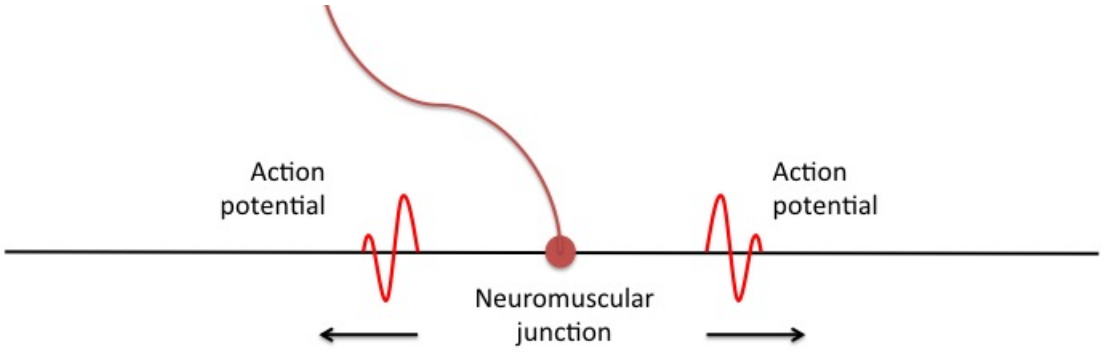

Figure 3.2: Muscle fibre action potentials are generated when a neural action potential is detected at the neuromuscular junction

The APs travel along the muscle fibre via changes in the potential between the inside and outside of the cell. The voltage distribution (in time) of the muscle fibre action potential was initially described mathematically as V_m by Rosenfalk [Rosenfalck, 1969], who defined the

equation

$$V_i(t) = \alpha \cdot t^3 \cdot e^{-\beta t} - \gamma \tag{3.3}$$

Equation 3.3 creates a distribution with the characteristic AP tripolar shape (Figure 3.3). α, β and γ are parameters describing the intracellular action potential. α is in v/s, β is in s^{-1} and γ is in volts. Altering α, β or γ dilates the AP waveform.

Merletti [Merletti et al., 1999a] extended upon this definition for $V_i(t)$, adding a scaling factor λ. As his work was in the space domain, the subsequent equation for V was given as

$$V_m(z) = A(\lambda z)^3 e^{-\lambda z} - B \tag{3.4}$$

λ has the effect of altering the timebase and amplitude of $V_m(z)$. A is the amplitude of the action potential, B is the resting membrane potential and z is the distance along the muscle fibre.

3.4 Current distribution of a muscle fibre action potential

The modelling of a single muscle fibre observed at a distance (skin surface) has been reported and used in many areas of EMG research. It is generally assumed that the muscle fibre is a line source where the diameter is neglected [Rosenfalck, 1969]. As a result of this assumption, the muscle fibre transmembrane ionic current can be described as the second spatial derivative of $V_m(z)$ [van Veen et al., 1993].

$$I_m(z) = C\frac{d^2V_m(z)}{dz^2} = CA\lambda^2(\lambda z)(6 - 6\lambda z + \lambda^2 z^2)e^{-\lambda z} \tag{3.5}$$

This distribution has the characteristic shape shown in Figure 3.3.

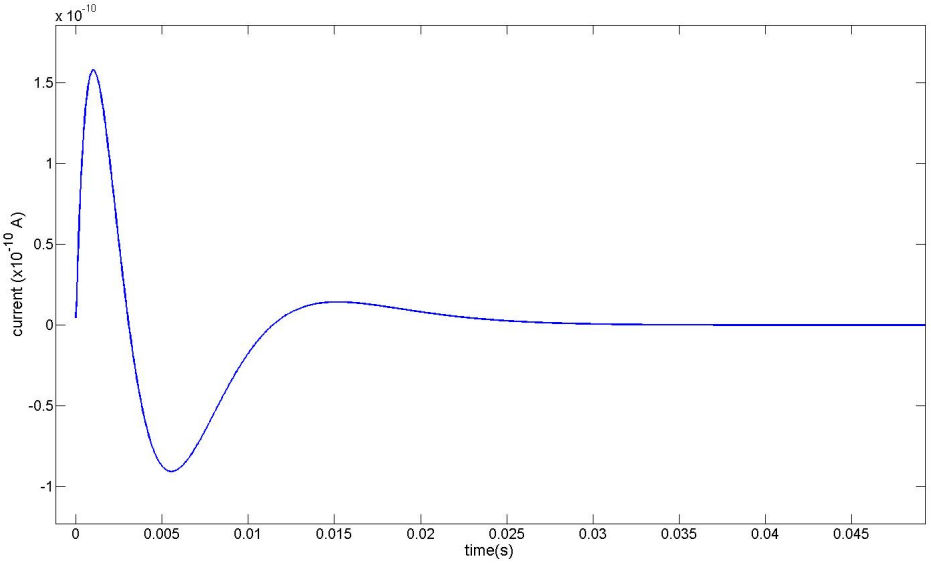

Figure 3.3: The muscle fibre action potential has a characteristic tripolar shape [van Veen et al., 1993]

In the work reported in this thesis, muscle fatigue is not considered. This means that the signal, and in particular the conduction velocity (v), is time invariant. It can therefore be assumed that $z = v \cdot t$. This allows the calculation of the current distribution in the time domain

$$I_m(t) = CA(\lambda v)^2(\lambda vt)(6 - 6\lambda vt + \lambda v^2 t^2)e^{-\lambda vt} \tag{3.6}$$

C is a constant that takes into account the conductivity of the fibre, σ_i , the muscle fibre conduction velocity, v, and the diameter of the muscle fibre, d [Rosenfalck, 1969, Lowery et al., 2000].

The majority of muscle models, particularly those of the biceps brachii, are modelled either without shape, or as a cylinder to approximate the fusiform muscle shape (refer to Figure 3.4).

The current distribution described by equation 3.6 defines the signal that would be mea-

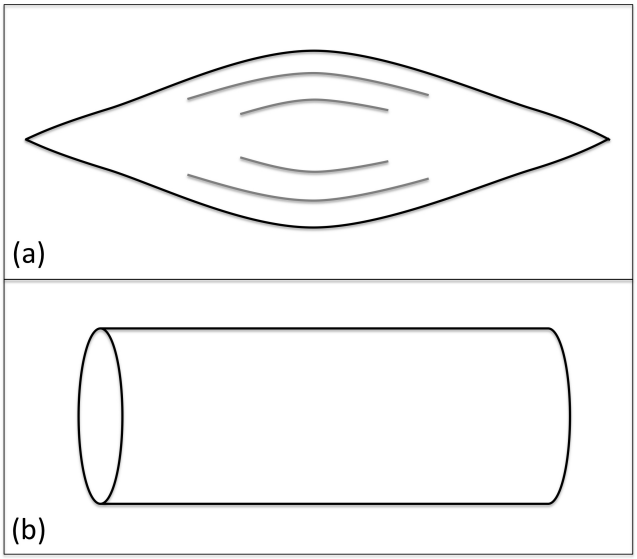

Figure 3.4: (a) The bicep muscle shape is fusiform; wide in the centre and tapering at each end. (b) Most bicep muscle studies approximate the muscle shape as a cylinder

sured by a needle electrode injected into a single muscle fibre. Further considerations for this model include

- Modelling many muscle fibres arranged into a number of motor units
- Modifying the signal to represent the changes due to the cutaneous tissue between the muscle fibre and the surface recording electrode

3.5 Volume conduction

The cutaneous tissue (fat and skin) through which the AP signal must pass in order to reach the recording electrode on the skin's surface has the effect of modifying the AP shape in a similar manner to a low pass filter. Therefore, the further the distance that the signal diffuses, the flatter and longer the AP current distribution will become.

The function $f(x, y, z)$ is introduced to simulate these changes to the AP signal [Plonsey, 1974].

$$f(x,y,z) = \frac{1}{4\pi\sigma_e}\frac{1}{\sqrt{(z-z') + \sigma[(x-x')^2 + (y-y')^2]}} \tag{3.7}$$

x, y and z are the co-ordinates of the point source.

σ_e is the extracellular conductivity, while σ is the ratio of the internal and external conductivities such that

$$\sigma = (\frac{\sigma_i}{\sigma_e})^2 \tag{3.8}$$

The convolution of the AP current distribution (Equation 3.6), with $f(x,y,z)$ (Equation 3.7), gives the action potential of a single muscle fibre as measured at the surface of the skin.

3.6 Modelling a motor unit

To model a motor unit (MU), rather than a single muscle fibre, the size of the MU must be considered. The size of a MU represents of the number of muscle fibres in the motor unit.

In this work, each motor unit is described by an equivalent muscle fibre, with an amplitude to indicate the MU size. This is an approximation. Future work should consider the fact that the muscle fibres in a MU are scattered about a defined territory and will thus have slightly different volume conduction properties.

A constant, K_m, is used to represent the motor unit size. The multiplication of the single muscle fibre AP by the constant K_m gives the signal of an active motor unit, as recorded at the surface of the skin.

A cross section of a muscle, showing a muscle fibre in a volume, the recording electrode on the surface of the skin and the spatial variables described in Figure 3.5. This image summarises the generation of the sEMG signal from a neural stimulating pulse.

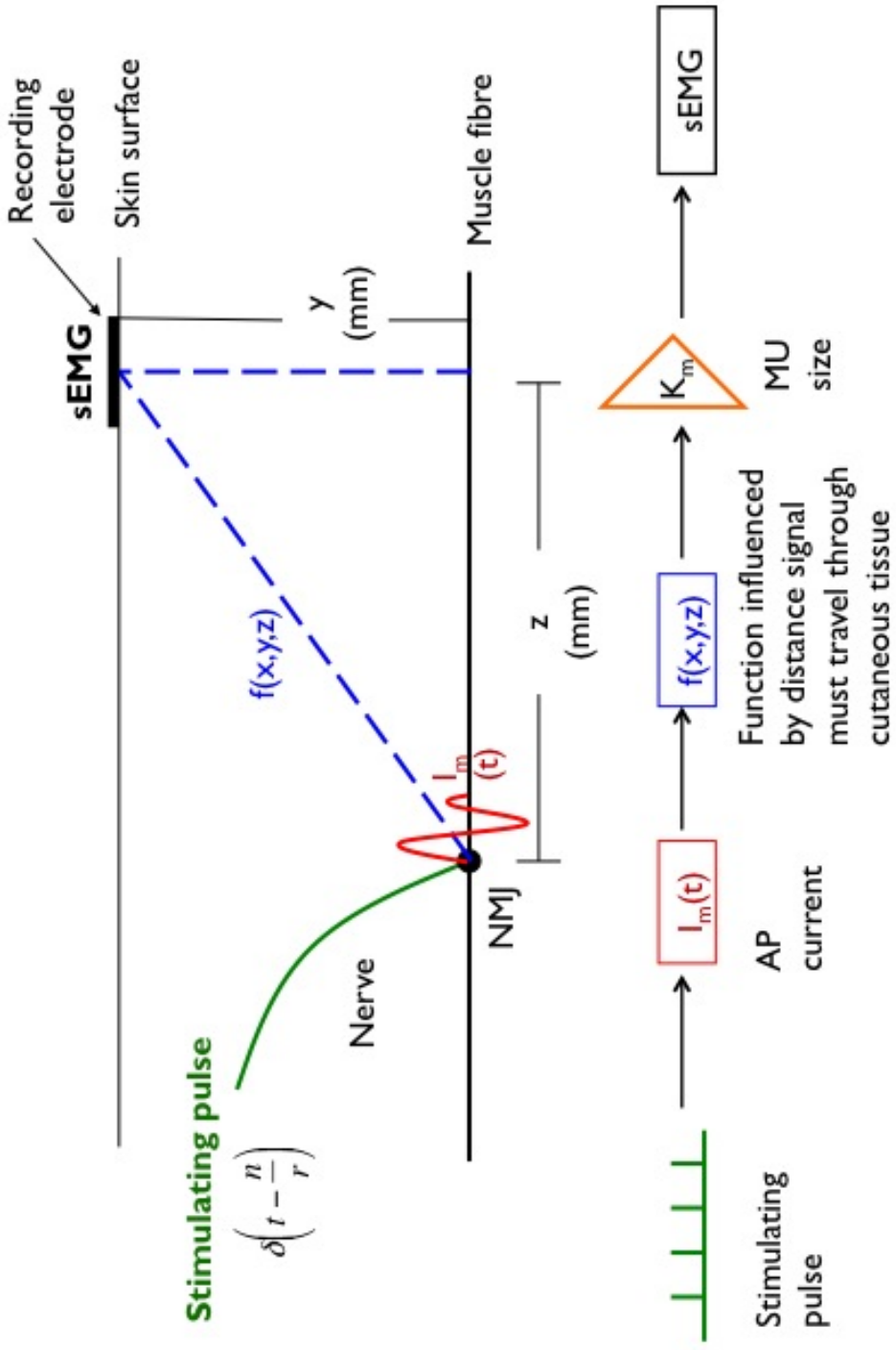

Figure 3.5: sEMG signal of a single muscle fibre

3.7 Modelling a whole muscle

To simulate the whole muscle, a number of motor units must be modelled simultaneously, where the superposition of their activation patterns gives the whole muscle sEMG.

The differences between each motor unit include

- conduction velocity
- firing frequency
- recruitment threshold
- size (number of fibres)
- position in the muscle body
- temporal offset of firing (τ_m)

As described in Chapter 2, the majority of muscle models use average values for these parameters, with most failing to consider the differences between slow and fast MU types. One of the novel features of the model implemented for this thesis work is that each motor unit has a unique value for each of these parameters, taken from distributions based on experimental data.

For the work reported here, the signals are time invariant, to represent non-fatigued muscles. Each MU is therefore assigned a unique, single conduction velocity (v) value, taken from a type-based distribution about an experimentally obtained mean. As described in section 3.2, each MU is given a distinct value of τ_m, taken from a random distribution. The size of each MU, K_m, is also a randomly assigned variable.

To increase the accuracy of the simulated sEMG signals to those found in-vivo, the recruitment threshold and firing frequency values are determined via a novel method.

3.8 A novel firing frequency and motor unit recruitment paradigm

In previous models, the AP firing frequencies of the motor units have been distributed about a common mean value or along a common linear distribution [Hamilton-Wright and Stashuk, 2005, Yao et al., 2000, Stashuk, 1993]. Thus, the slow and the fast fibre types have been assigned the same range of firing frequencies values. However, experiments have shown that the firing frequencies of type I muscle fibres are lower than those of type II [Duchene and Hogrel, 2000]. In addition, the force at which the MU is recruited is dependent on the MU type.

Work by Gydikov [Gydikov and Kosarov, 1974] showed that the firing frequencies of type I and type II fibres are significantly different, and the muscle force at which the motor units are recruited is dependent on the motor unit type. At low force levels only type I fibres are active, with firing rates distributed about averages of 8-14 Hz. At higher force levels, type II fibres are also active, at firing rates of 12.5 to 24.5 Hz.

To increase the physiological accuracy of this model, distributions of possible values for the recruitment threshold and MU firing frequency of each motor unit were developed, based on the experimental results of Gydikov. Both parameters were assigned probabilities based on muscle fibre type, so that type I fibres are recruited at low force levels, and type II fibres are recruited with increasing force. Similarly, the firing rate of each motor unit is type based.

A sample of the firing rates and recruitment thresholds of a pool of 110 MUs is shown in Figure 4.7. Slow motor units are represented in red, while fast motor units are represented in blue. It is clear that at a low force level (e.g. 20% MVC), only slow muscle fibre types are active, and they have low firing rates. At high force levels, both MU types are active, and the firing frequencies range from 12-24 Hz.

It should be noted that although this paradigm reflects the work of Gydikov and other, related studies, recent work has used sEMG signal decomposition to revisit the relationship. De Luca and Hostage found that although the relationship between force level and firing frequency range is similar to that found by Gydikov, in some muscles of the hu-

man body, recruitment threshold has an inverse relationship with the initial firing frequency [DeLuca and Hostage, 2010]. An in depth evaluation of recent decomposition studies should be conducted ahead of future sEMG modelling work.

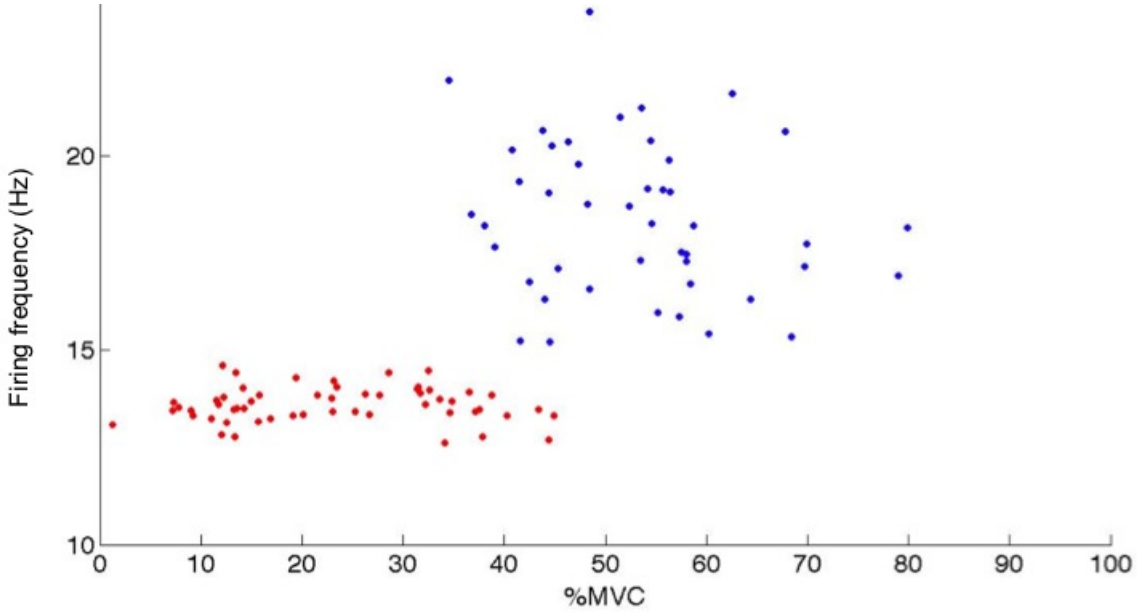

Figure 3.6: Recruitment thresholds (%MVC) and average firing frequencies (Hz) of a pool of 110 motor units. Red represents slow fibre motor units, blue represents fast fibre motor units.

3.9 Modelling the muscle force output

To ensure that the sEMG model can be accurately validated against experimental data, a second output was added. As well as simulating an sEMG signal, it was decided to also simulate the force output of a skeletal muscle contraction.

The implementation of a force output here is based on the work by Fuglevand, who described a model with both sEMG and force outputs [Fuglevand et al., 1993]. The force output of a muscle is dependent on the number of active motor units and the size and firing rate of each of these MUs. This implementation therefore differs from Fuglevand as the force is based on the novel firing rate and recruitment strategies described in section 3.8.

A muscle fibre twitch is the mechanical event generated in a single MU in response to an action potential from the stimulating neuron. The twitch response for a single motor unit is given by

$$g(t) = \frac{P \cdot t}{T} e^{1-(t/T)} \tag{3.9}$$

where P is the peak amplitude of the twitch force and T is the rise time to reach the peak force.

As the biceps brachii is a fusiform muscle, the force can be modelled approximately as a summation of the twitch force of each active MU in the MU pool. The MU twitch from a motor unit in a pool of active MUs, is therefore described by

$$g_i(t) = \frac{P_i \cdot t}{T_i} \cdot e^{1-(\frac{t}{T_i})} \tag{3.10}$$

where i is the MU number.

The force output of a motor unit is equivalent to the sum of impulse responses, given by

$$F_i(t) = \sum_{j=1}^{k} g_{ij}(t - t_{ij}) \tag{3.11}$$

The muscle force output can then be expressed as the summation of all active MU force outputs

$$F_m(t) = \sum_{i=1}^{n} F_i(t) \tag{3.12}$$

The peak twitch amplitude, P, of each MU is related to its recruitment threshold and distributed such that the last recruited MU has a peak amplitude 100 times that of the first

recruited MU. The peak twitch amplitudes are distributed according to

$$P_i = e^{(\frac{RP}{n})\cdot i} \tag{3.13}$$

where RP is the range of peak values (100 in this case), and n is the number of MUs.

A histogram of the peak twitch amplitudes for a pool of 110 MUs is shown in Figure 3.7.

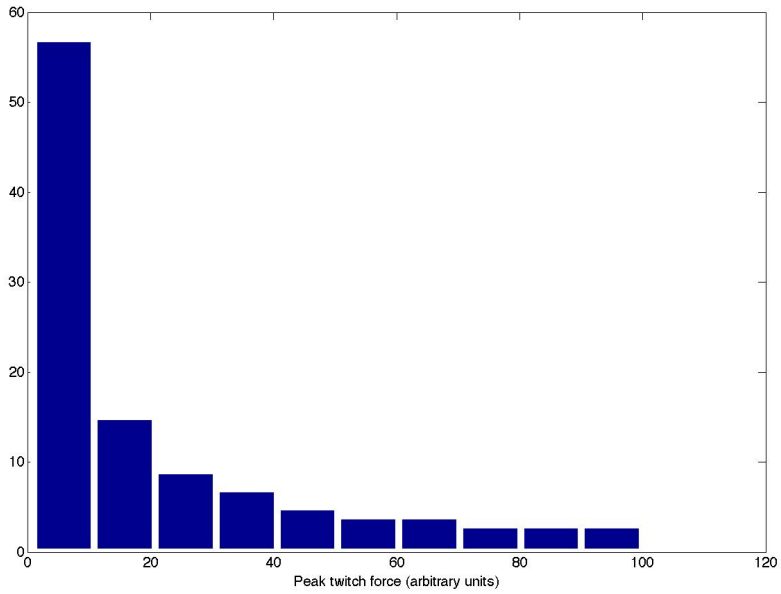

Figure 3.7: Histogram showing the number of motor units in each range of peak twitch amplitude

The contraction time of the twitch force is related to the peak amplitude. For each MU, the contraction time, T_i, is given by

$$T_i = 90 \cdot (\frac{1}{P_i})^{1/log_3 RP} \tag{3.14}$$

The log is base 3 as the range of contraction times is 3-fold. 90 represents the longest contraction time in the MU pool.

These parameters are modified by a gain value, introduced to model the non-linearity of

the force with stimulus rate. This relationship was investigated by Bigland (Bigland1954), who plotted the non-linearity between isometric force and the stimulation rate. The gain is dependent on the firing rate of each MU.

The total force exerted during a contraction is the summation of the contributing force trains from each active MU.

3.10 Conclusions

This chapter has described a novel sEMG/force model which simulates the surface electromyogram signal and the mechanical force generated by a contracting skeletal muscle. The model simulates the neural input signal, the subsequent contraction of muscle fibres, and the effect of volume conduction on the signal detected at the surface of the skin.

The novel features of the sEMG/force model include

- Population with parameter values from distributions based on experimental results
- Type based parameter values which allow type I and type II muscle fibres to be simulated independently
- Introduction of an experimentally-based firing frequency and motor unit recruitment strategy

In addition, a second model output has been added. This force value provides more information to the experimentalist, and allows the model to be validated with more strength than a single output design. As described, this implementation of the force output is based on the model described by Fuglevand. However, the calculated twitch force is dependent on the recruitment order and the firing rate of each motor unit in the active MU pool. These parameters are based on the novel distribution described in section 3.8.

An accurate sEMG/force model is a useful tool for studying the neuromuscular system, particularly with regards to changes from the norm. Before it can be utilised for such a purpose, the signals simulated by the model must be verified against experimental results.

Chapter 4 describes the experimental method followed to acquire experimental data and the results of the validation process.

Chapter 4

Experimental and Simulation Methods

This chapter is divided into two main sections. Section 1 details the experimental procedures used to obtain surface electromyogram (sEMG) data from human experiments. Section 2 describes the methods followed to populate, simulate and verify the sEMG/force model described in Chapter 3.

4.1 Experimental methods

4.1.1 Surface electromyogram

To verify a biological model, real life data is required. The data used to verify the accuracy of the sEMG/force model was acquired from a series of human experiments. 10 young adult male subjects performed isometric contractions of the bicep muscle and the brachiradialis muscle at varying levels of intensity. To acquire the data used in the ageing study in Chapters 5 and 6, subjects of varying ages contracted the bicep muscles at maximum effort.

The experimental protocols followed to obtain these two data sets are described in this section.

4.1.2 General protocol

4.1.2.1 Skin preparation

Firstly, the electrode sites were located. The electrodes to record from the bicep braccii were placed on the anterior of the arm above the biceps, on either side of the line between the anticubital fossa (depression in the front of the elbow - lateral to the biceps braccii tendon) and the acromion process (part of the scapula which extends over the shoulder), at 1/3 from the anticubital fossa [Cram et al., 1998, Seniam, 2009] The electrodes to record from the brachioradialis muscle were placed on the line between the lateral styloid process and the lateral epicondyle, at 1/3 from the lateral epicondyle.

A body current return electrode was affixed above the olocranon process of the ulna bone at the elbow joint. Prior to electrode placement, the skin was cleaned and abraded with alcohol wipes to reduce skin impedance and ensure adequate adhesion of the electrodes. If the electrode sites were hairy, the skin was shaved with a disposable razor.

4.1.2.2 Electrodes

SEMG signals were recorded using Delsys (Boston, MA, USA); a proprietary sEMG acquisition system. The system supports bipolar recording and has a gain of 1000, CMRR of 92 dB and bandwidth of 20-450 Hz, with 12dB/octave roll-off. The sampling rate was fixed at 1000 samples per second, and the resolution was 16 bits/ sample. Delsys bipolar electrodes were used. These are active electrodes with two silver bars (1 mm wide and 10 mm long) mounted directly on the preamplifier with a fixed inter-electrode distance of 10 mm.

Two pairs of differential electrodes were placed on the selected muscles, at the locations

Figure 4.1: The skin above the bicep muscle was cleaned with an alcohol wipe

described in section 4.1.2.1. The two pairs of electrodes lay parallel to one another, in the direction of the muscle fibres (refer to Figure 4.2). The electrode cables were taped to the skin at distance from the electrode site, to ensure that the weight of the leads did not alter the recorded signal.

The recording and reference electrodes were connected to the Delsys wireless box for transmission over wireless local area network (WLAN) to the computer.

4.1.2.3 Muscle contraction

To record experimental data from the biceps braccii, participants were seated in a sturdy and adjustable chair with their feet flat on the floor. The upper arm was rested on the surface of a desk, in a horizontal position with the palm facing upward. The elbow was fixed at 90 degrees, with the fingers in line with a wall mounted force sensor (S-type force sensor - INTERFACE SM25) attached to a wrist strap held loosely in the hand (Figures 4.3 and 4.4). The output of the force sensor was recorded on an unused channel of the sEMG acquisition system and displayed in real time. The subjects were asked to pull their fingers back towards the upper

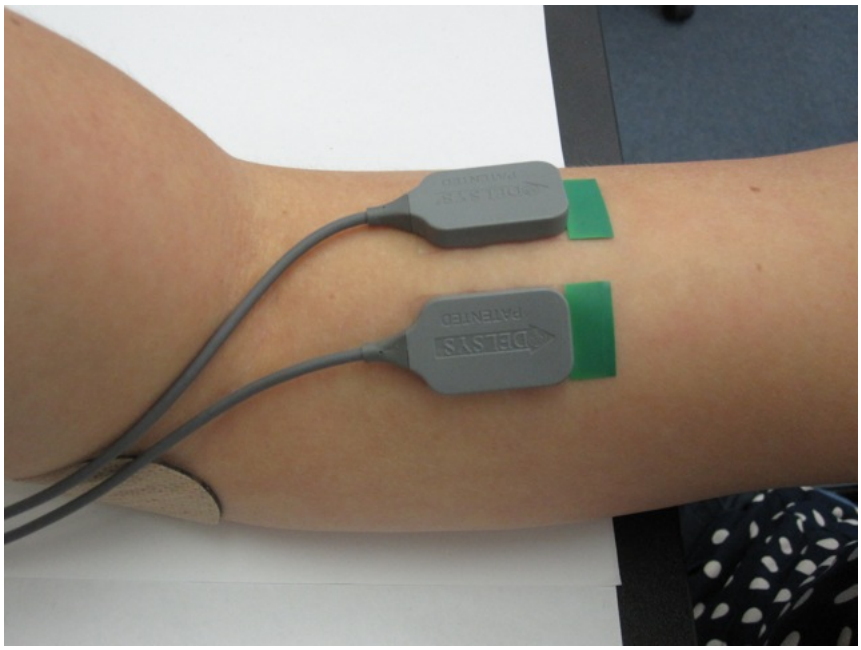

Figure 4.2: The placement of electrodes to record bicep muscle contractions

arm. Resisted by the wrist strap, this movement resulted in an isometric flexion of the biceps brachii.

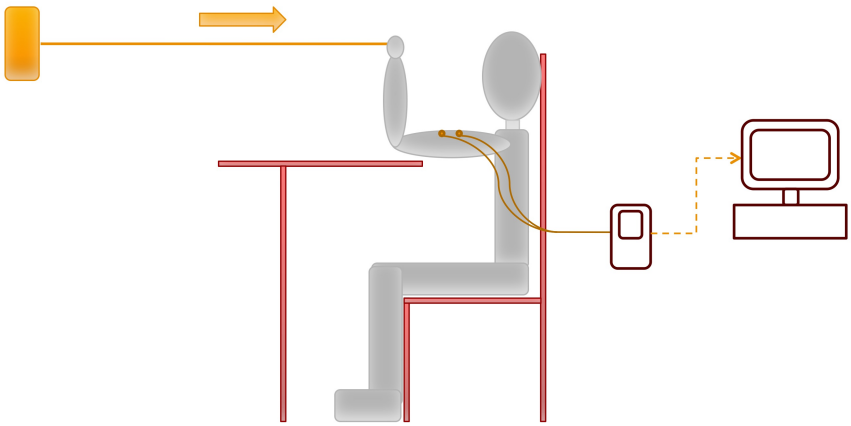

Figure 4.3: The position of the subject during elbow flexion experiments

To record from the brachioradialis muscle, a similar process was followed. However, the forearm was rotated to be midway between pronation and supination. The hand was placed through the wrist strap so that the fingers were perpendicular to the wall. This arm position

Figure 4.4: The position of the subject and equipment during elbow flexion experiments (note that the fingers are horizontally aligned with the force sensor)

reduces the contraction levels of surrounding muscles and increases the contraction of the brachioradialis [Calder et al., 2008].

4.1.3 Surface electromyogram model verification experimental protocol

This section describes the specific protocol followed to acquire the experimental data used to verify the sEMG model. Ten healthy male participants, with no history of neuromuscular disease or injury participated in this work. The results of the study are included at the end of this chapter.

4.1.3.1 Maximum voluntary contraction

The maximum voluntary contraction (MVC) is a standard method used to generate muscle contractions of comparable effort between subjects. The first stage is to determine the maximum muscle force achievable during a voluntary contraction.

Each subject was asked to perform the contraction described in section 4.1.2.3 with as much force as they could whilst maintaining a controlled movement and correct body position. The participants were given visual feedback of the force of contraction and provided with verbal encouragement to assist them in maintaining constant, maximum force. This maximum contraction was held and recorded for 5 seconds.

This was repeated three times, with two minutes rest between each iteration. In each case, the output from the force sensor was acquired. The average force across the three contractions was the MVC for that muscle.

The MVC was measured for both the biceps and brachioradialis muscles of each subject. Force sensor output values corresponding to 30%, 50% and 80% MVC were then calculated.

4.1.3.2 Acquisition of bicep data

Ten seconds of data was required at each contraction level. As shown in Figure 4.5, subjects generally need 2-3 seconds to reach and maintain the desired force level. The subjects were therefore asked to hold each contraction for 15 seconds, so that a ten second segment with constant force could be used for analysis.

After each 15 second contraction, the subject rested for 60 seconds to ensure the muscles did not become fatigued. The contractions were conducted in sets of three, where the first two sets were in the order of 80%, 50%, then 30% MVC. For the final set, the order was changed to 30%, 50%, then 80% MVC, to ensure that the order did not influence the results.

During the contractions and rest periods, surface electromyogram and mechanical force

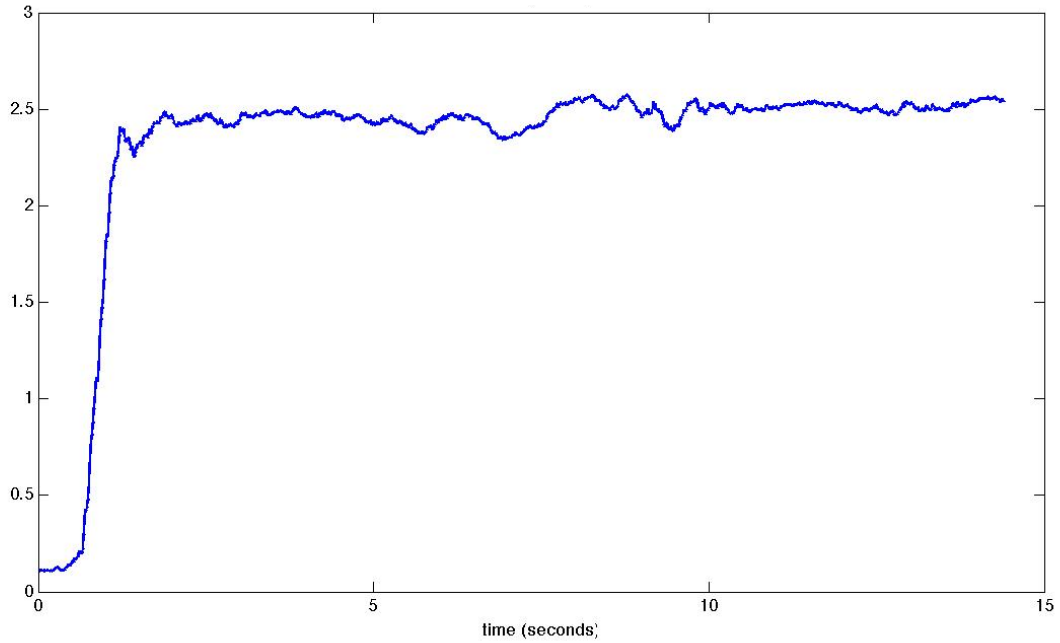

Figure 4.5: The force (in arbitrary units) acquired by the wall mounted force sensor during a sustained bicep contraction

parameters were recorded. Figure 4.6 shows an example of the sEMG and force signals acquired during a typical contraction. The methods used to process the acquired data are described in section 4.2.5.

4.1.3.3 Acquisition of brachioradialis data

Each of the ten subjects also undertook contractions of the brachioradialis muscle. The procedures followed were the same as those outlined in section 4.1.3.2, except that the hand was rotated 90 degrees so that the palm was perpendicular to the wall.

Once again, the subjects completed three sets of isometric contractions at 30%, 50% and 80% MVC. The surface EMG and force signals were recorded and analysed.

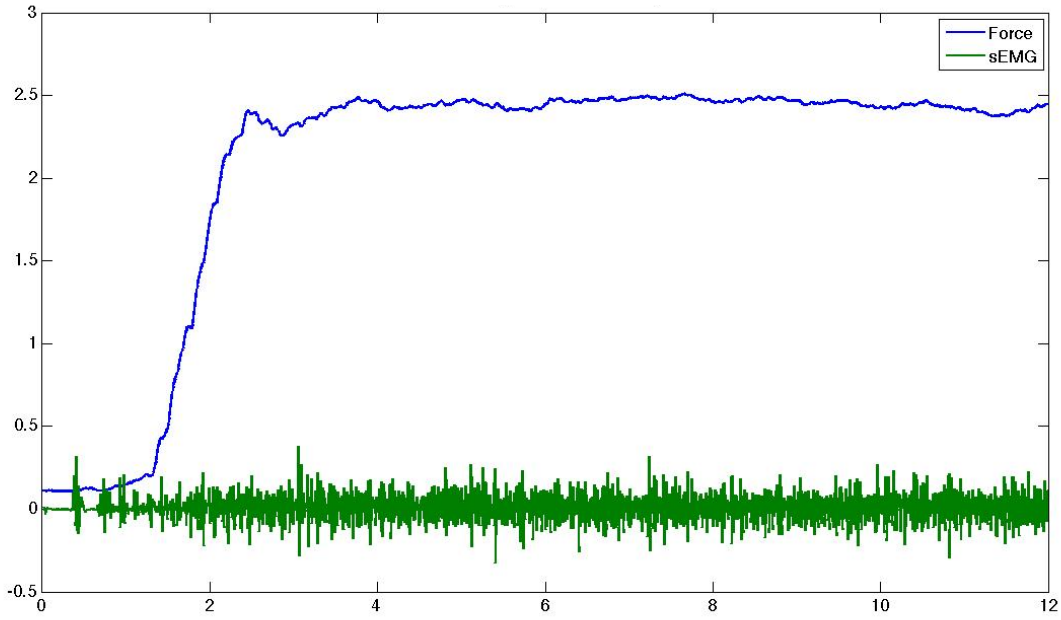

Figure 4.6: A typical signal set recorded during bicep muscle contractions. This figure shows the force and the sEMG, both in unnormalised voltage units.

4.1.3.4 Limitations of this experimental protocol

It must be acknowledged that no muscle can be contracted in isolation. Movements were selected which increase the contraction of the muscles of interest, and the body position of the subject was chosen to minimise the contraction of surrounding muscles. However, to the author's knowledge, the contributions of the four muscles (Section 2.2.7) that generate elbow flexion are not known. This is a limitation of this work as the force contraction of an individual muscle may not vary linearly with the force measured.

4.1.4 Ageing study experimental protocol

For the experimental data used in Chapter 5, thirty healthy subjects, with no history of neuromuscular disease or injury participated. The subjects were divided into two groups:

- Group 1: Younger - 16 subjects; age range 20-28 years

- Group 2: Older - 14 subjects; age range 60-69 years

Each subject contracted the bicep muscle to their maximum effort for 10 seconds. The participants were given visual feedback of the force of contraction and provided with verbal encouragement to assist them in maintaining constant, maximum force. During the contractions, both the sEMG and the force outputs were measured.

The first 5 seconds of data from each subject (during the non-fatigued state) where the force was held steadily were extracted.

4.1.5 Signal processing

To compare signals from the sEMG model with experimental data, a number of signal features were calculated. Each of these features are widely used in the characterisation of sEMG signals and reveal information about the contraction level of the muscle and firing frequency and AP shape of the motor units. Root mean square (RMS) and mean absolute value are related to the amplitude features of the signal. Mean power frequency (MNF), zero crossing (ZC) and waveform length describe the frequency distribution of the sEMG.

Time varying features such as wavelets and time-frequency analysis were not studied because this model is time invariant.

- Root mean square (RMS) [Oskoei and Huosheng, 2008]

  The RMS of an EMG signal represents the amplitude and in the non-fatigued state, is associated with the force exerted by the muscle.

$$RMS = \sqrt{\frac{\sum_{i=1}^{N} x_i^2}{N}} \tag{4.1}$$

  To eliminate the effects of varying body size and composition, the RMS results in the ageing study were normalised against the body mass index (BMI) of each subject.

- Mean power frequency (MNF)

  The mean power frequency is a spectral feature that allows changes in the spectrum of the signal to be tracked. It is calculated by firstly finding the power spectral density (PSD) of the signal. The PDF was calculated to a 95% confidence interval in this work. If F is the maximum frequency of the signal, then the power, P is given by;

$$P = \int_0^F PSD(f)df \tag{4.2}$$

  The probability function at a given frequency, f, is;

$$p(f) = \frac{PSD(f)}{P} \tag{4.3}$$

The mean power frequency can then be found by;

$$MNF = \int_0^F p(f) f df \tag{4.4}$$

- Zero crossings per second (ZC)

  The zero crossings (ZC) feature is calculated by summing the number of times that the curve crosses the zero am-plitude axis. It is indicative of both the average frequency of the signal, and of the extent to which MUAP firings are synchronised with one another. It was calculated using;

$$ZC = \sum_{i=1}^{n} sign(-x_i x_{i+1}) \tag{4.5}$$

  where

$$sign(x) = \begin{cases} 1 & \text{if } x >= 0 \\ 0 & \text{otherwise.} \end{cases}$$

4.2 Simulation methods

The model presented in this thesis is more versatile and accurate than others in the field as it simulates multiple muscle fibre types, is populated by physiologically accurate motor unit properties and can be validated experimentally by both electrical and mechanical output signals. This section describes the implementation and validation of this sEMG model.

4.2.1 Surface electromyogram/force model implementation

The model presented here simulates both a whole muscle electromyogram signal, as measured on the surface of the skin, and the force output of a contracting muscle. The model is described

in detail in Chapter 3.

4.2.2 Model input parameters

The model covers four stages of EMG generation; neuronal stimulating pulse, muscle fibre action potential, motor unit action potential and surface EMG simulation. This model simulates a lifelike muscle by introducing random elements to give distributions of parameters, rather than single values. Parameters defined by a distribution include the MU size, the firing rate, initial temporal offset and the muscle fibre conduction velocity. The distributions used are based on mean and standard deviation values as reported in the literature. The model parameters used for each muscle are outlined in Table 4.1. Additional variables are shown in Table 4.2.

Parameter	**BB**	**BR**
Number of active motor units (MU) at 100% MVC	110	100
Average conduction velocity $m.s^{-1}$ [Krogh-Lund and Jrgensen, 1992]	4.3 ± 0.29	4.2 ± 0.41
Conduction velocity (fast fibres) [Farina et al., 2002b]	4.9 ± 0.3	4.9 ± 0.3
Conduction velocity (slow fibres)	3.9 ± 0.3	3.7 ± 0.3
Percentage of type 1 fibres (%) [Kukulka and Clamann, 1981, Krogh-Lund and Jrgensen, 1992]	45	40

Table 4.1: Parameters used for EMG model simulation of the biceps braccii (BB) and the brachioradialis (BR) (For each parameter, the ± value represents the standard deviation of the distribution)

Parameter	Value
Muscle fibre diameter [van Veen et al., 1993]	25 μm
Depth of MU from surface [Roeleveld et al., 1997]	35 mm ± 2mm
Duration of AP along fibre [Dumitru et al., 1999]	16 mm
Cutaneous tissue [Roeleveld et al., 1997]	Single, isotropic, 3 mm layer
Muscle half-fibre length [Farina et al., 2002b]	65 mm
Simulation sampling frequency	10000 Hz

Table 4.2: Additional parameters used for EMG model simulation of the biceps braccii (BB) and the brachioradialis (BR)

4.2.3 An accurate motor unit recruitment strategy

Needle electrode studies have determined that motor units exhibit characteristic thresholds, which determine the order in which they are recruited for contraction. Generally, type I MUs are recruited at lower thresholds than type II MUs. In addition, the firing frequency of MUs depends upon the MU type. In low-level isometric contractions of the biceps brachii, Gydikov found that only type I fibres were active, and that they were firing at an average rate of 8-14 Hz. At higher force levels (greater than 40% of the maximum voluntary contraction), type II fibres were also active, at firing rates of 12.5 to 24.5 Hz, increasing with force [Gydikov and Kosarov, 1974].

This implementation of this model incorporates recruitment thresholds and variable MU firing frequencies developed from Gaussian distributions of the results described by Gydikov. A sample of the firing rates and recruitment thresholds of a set of 100 active MUs is shown in Figure **??**. The type I motor units are plotted in red and the type II motor units in blue.

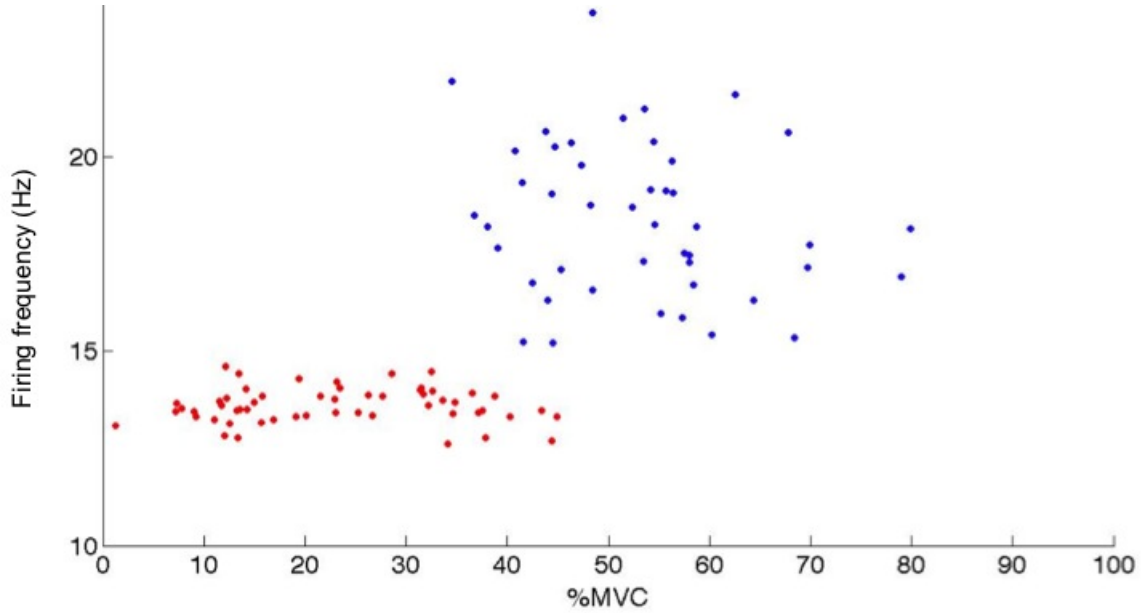

Figure 4.7: Recruitment thresholds (%MVC) and average firing frequencies (Hz) of a pool of 110 motor units. Red represents slow fibre motor units, blue represents fast fibre motor units.

4.2.4 Surface electromyogram and muscle force outputs

To allow simulated signals to be compared with experimentally obtained surface EMG signals, the total number of MUs are considered, rather than a single MU. The summation of the contributions of each active motor unit gives the whole muscle sEMG signal.

In addition, the model developed for this research includes a second output; the force signal. The force output by a contracting muscle is dependent on the number of active motor units and the size and firing rate of each of these MUs. The implementation of the force output here is based on the work by Fuglevand [Fuglevand et al., 1993], who described a model with both sEMG and force outputs. As the muscle fibres in the biceps brachii run approximately parallel to the direction of muscle pull, the force can be modelled as a summation of the twitch force of each active MU in the MU pool.

The peak twitch amplitude, P, of each MU is related to its recruitment threshold and distributed such that the last recruited MU has a peak amplitude 100 times that of the first recruited MU. The contraction time of the twitch force is related to the peak amplitude, as described in [Fuglevand et al., 1993]. The firing rate of each twitch is determined by the motor unit firing rate. As described in section 4.2.3, the MU firing frequency is based on a novel distribution scheme developed for this work.

The force output calculations are described in detail in Chapter 3. The validation of both the mechanical and electrical outputs of the sEMG/force model to experimental data is summarised in the remainder of this chapter.

4.3 Validation of surface electromyogram model

In order to use the sEMG/force model to study muscle contraction and changes in muscle physiology, it must be shown to generate accurate and useful simulated biosignals. This section describes work done to validate the sEMG/force model against experimental data.

4.3.1 Validation of model versatility

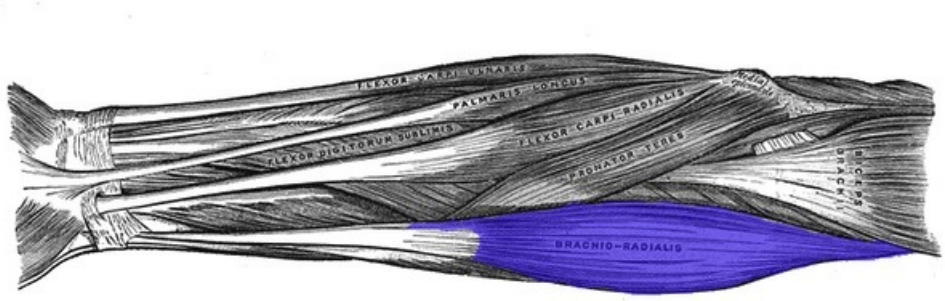

Figure 4.8: The location of the brachioradialis muscle (Reproduced from [Gray, 1973])

The first step was to to verify the versatility of the EMG model. The model would be most useful if it were capable of simulating different muscles of the human body. For each of these muscles, the model should be capable of simulating the sEMG signal at varying contraction strengths.

To test the versatility, two different skeletal muscles were studied; the brachioradialis in the forearm (refer to Figure 4.8) and the biceps muscle in the upper arm (refer to Figure 4.9). Experiments were conducted to compare simulated signals with experimental data at varying force levels.

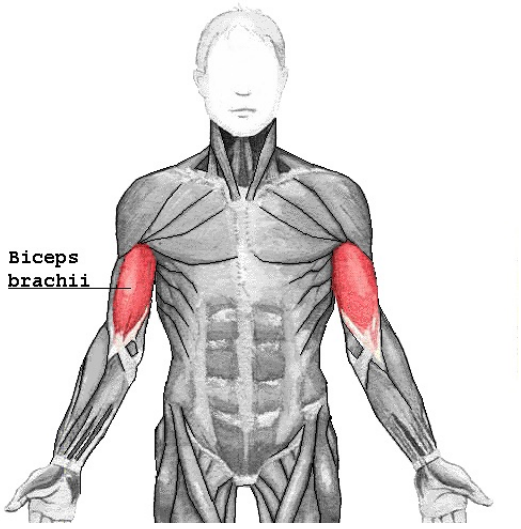

Figure 4.9: The location of the biceps brachii muscle ((c) [Johansson, 2005])

SEMG signals were generated simulating the biceps bracii and brachoradialis muscles of an average adult undergoing isometric contractions at 30% and 50% maximum voluntary contraction (MVC). Ten simulations were run for each case.

To verify the simulated results, experiments were conducted on the biceps brachii and brachioradialis of a healthy human subject. The experimental methodology was detailed in section 4.1.3. The RMS, ZC and MNF were calculated from both the experimental and simulated data sets for the brachioradialis (Table 4.3) and the biceps muscles (Table 4.4).

Feature	50%MVC		30%MVC	
	Simulation	Experiment	Simulation	Experiment
RMS	0.016 ± 0.0016	0.015 ± 0.008	0.0076 ± 0.014	0.0089 ± 0.0006
ZC	156 ± 5	164 ± 5	157 ± 4	165 ± 15
MNF	73 ± 2	73 ± 5	73 ± 1	73 ± 4

Table 4.3: Average values for features of the brachioradialis sEMG signal calculated from simulated and experimental data (± standard deviation)

Feature	50%MVC		30%MVC	
	Simulation	Experiment	Simulation	Experiment
RMS	0.036 ± 0.012	0.044 ± 0.0046	0.024 ± 0.007	0.028 ± 0.0008
ZC	121 ± 8	147 ± 9	125 ± 18	150 ± 6
MNF	58.36 ± 2	60.58 ± 8	61.34 ± 5	63.40 ± 1

Table 4.4: Average values for features of the bicep sEMG signal calculated from simulated and experimental data (± standard deviation)

The RMS and MNF for each contraction type are plotted in Figures 4.10 and 4.11.

From Tables 4.3 and 4.4 as well as Figures 4.10 and 4.11 it was observed

- The average RMS increases with both muscle size and contraction strength
- The average RMS is similar between experimental and simulated data for all contraction types
- Zero crossing values between data sets are similar. The number of zero crossings per second changes between the different muscles, but does not change with contraction strength.

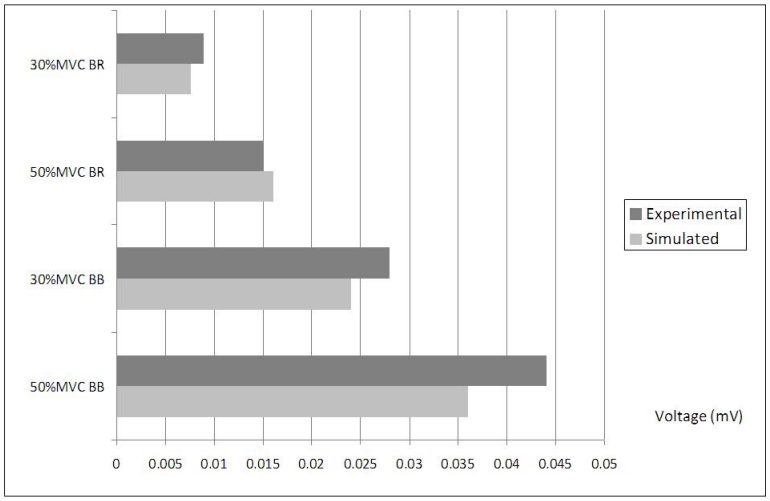

Figure 4.10: The average RMS calculated for each contraction level for the biceps bracii (BB) and brachioradialis (BR) muscles

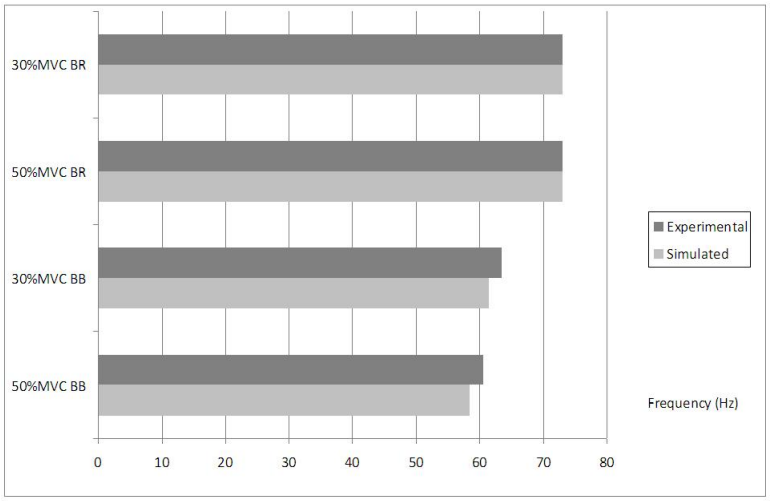

Figure 4.11: The average MNF calculated for each contraction level for the biceps bracii (BB) and brachioradialis (BR) muscles

- The MNF is also consistent between simulated/experimental data and across contraction levels, but varies between the different muscles.

It should be noted, as observed in section 4.1.3.4, that although 30% and 50% of MVC (force) was achieved during these experiments, it is not certain that the individual muscles of interest were contracting at these ratios.

4.3.2 Validation of novel recruitment strategy

In the majority of reported sEMG models, the firing frequencies of the motor units have been distributed about a common mean value, meaning that slow and fast MU types have the same range of firing frequencies values. In previous work by the candidate [Wheeler et al., 2010b] the fast and slow muscle fibre types have been modelled independently, with firing frequency values distributed about a pair of representative mean values.

This model improved on this strategy, incorporating recruitment thresholds and variable MU firing frequencies developed from the results described in [Gydikov and Kosarov, 1974]. This novel recruitment and firing frequency strategy is described in detail in section 4.2.3. The model was simulated using the muscle parameters outlined in Tables 4.1 and 4.2, in conjunction with the novel recruitment and firing frequency strategy.

The simulated signals were then compared with experimental results. Ten healthy male subjects were asked to perform isometric contractions for 10 seconds at 30%, 50% and 80% maximum voluntary contraction (MVC). The RMS was calculated on both simulated and experimental data. Figure 4.12 shows the RMS varying with muscle force.

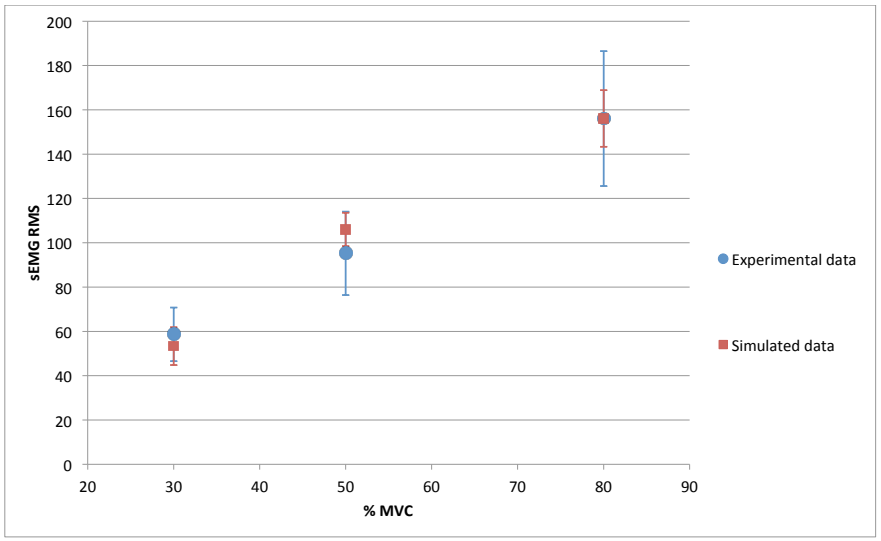

Figure 4.12: Average RMS values across 10 subjects at each force level for experimental and simulated data

4.3.3 Validation of dual outputs

To avoid the risks of self-validation, the model required a second output to verify the accuracy of simulations against real life results. It was decided to add an output signal to represent the force of a muscle contraction. The calculations leading to the generation of this signal are described in Chapter 3. The result of these calculations is a signal sampled at 10000 Hz representing the summation of the twitch forces of all active motor units.

To validate the sEMG and force model outputs, the amplitudes of the simulated signals at varying contraction levels were compared with experimental results. For this purpose, experimental and simulation experiments were conducted on the biceps brachii of 10 healthy human subjects.

For both experimental and simulated data, three recordings were obtained at each of three contraction levels; 30%, 50% and 80% MVC. The RMS of sEMG and the force output were averaged across the three trials in each case. The magnitude of the simulated data was normalized to match the experimental data at 80% MVC, where all motor units in the biceps brachii are active.

Figure 4.13 shows the average RMS of sEMG across all 10 subjects for each contraction level. The error bars show the standard deviation of the data from this mean value. A linear trendline has been fitted to this data. As expected, the relationship between sEMG RMS and %MVC is an linear relationship. The gradient of the sEMG RMS/% MVC trend lines for each of the ten subjects are shown in Table 4.5 (a) and Table 4.5 (b) shows the accuracy of the linear fits.

The RMS of the experimental and simulated force outputs were also compared. The averages for all ten participants are plotted in Figure 4.14.

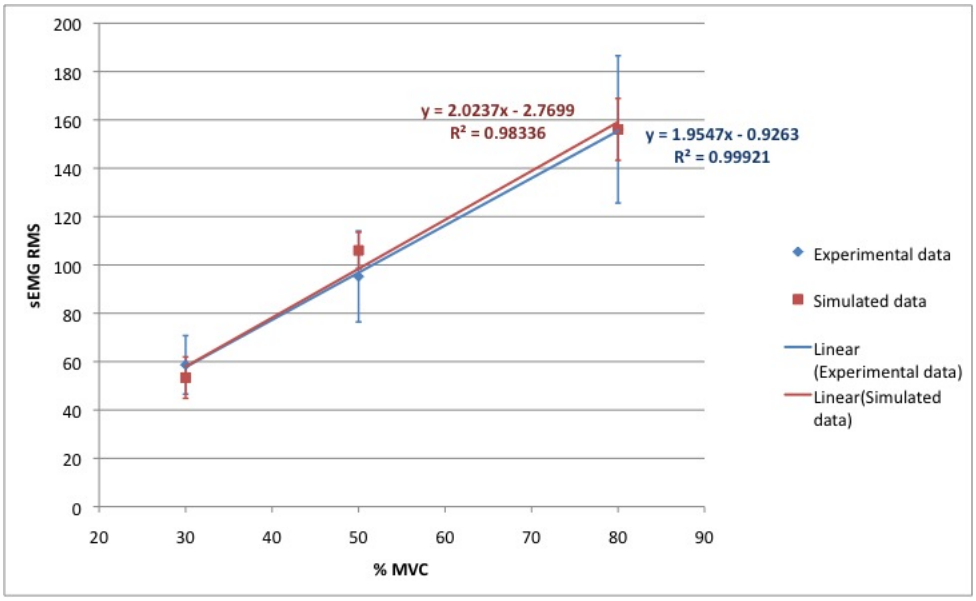

Figure 4.13: Average RMS of simulated and experimental data sets, increasing with %MVC. The amplitudes of the experimental RMS values are in arbitrary voltage units. The amplitudes of the simulated data were normalised to match the experimental results at 80% MVC.

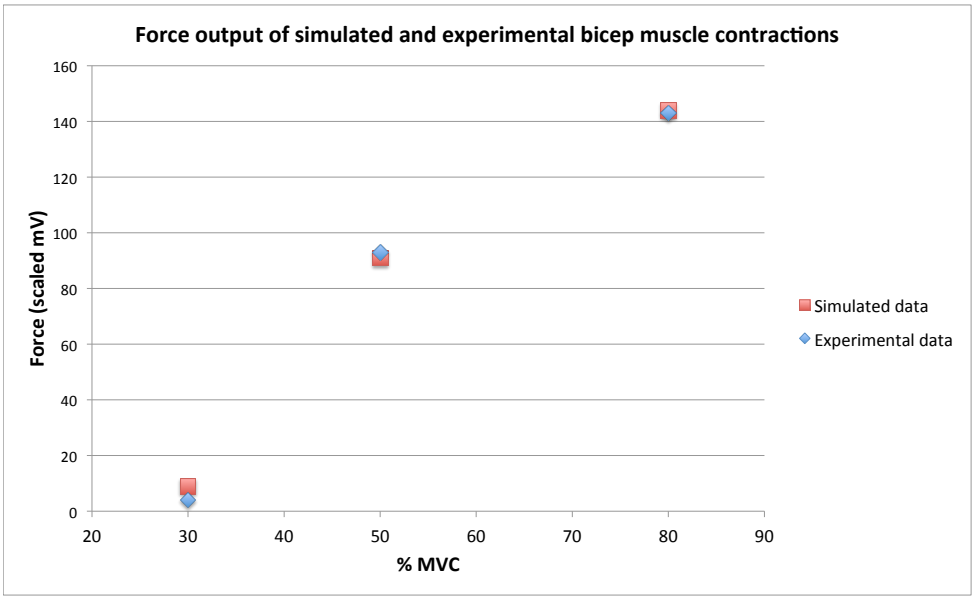

Figure 4.14: RMS of the average force for 10 subjects

(a)	Experimental	Simulated
Subject 1	2.3520	2.6210
Subject 2	2.1063	1.7660
Subject 3	2.0894	1.5992
Subject 4	2.2177	2.1698
Subject 5	2.0173	2.4225
Subject 6	2.1411	1.3087
Subject 7	2.0157	1.7111
Subject 8	1.8024	1.2667
Subject 9	2.2344	2.1117
Subject 10	1.8387	1.9923
(b)	Experimental	Simulated
Subject 1	0.9985	0.9966
Subject 2	0.9999	0.9574
Subject 3	0.9994	0.8516
Subject 4	0.9987	0.9999
Subject 5	0.9954	0.9719
Subject 6	0.9998	0.9993
Subject 7	0.9801	0.9997
Subject 8	0.9789	0.9999
Subject 9	0.9999	0.9921
Subject 10	0.9992	0.9233

Table 4.5: (a) Rate of change of RMS with force (MVC). (b) Accuracy of linear fit for rate of change of RMS (R2 value).

4.3.4 Discussion on the validation of the sEMG/force model

An adaptable model to simulate the surface EMG and muscle force signals of a contracting muscle was developed, integrating the single fibre models reported previously [Rosenfalck, 1969] [Merletti et al., 1999a] [Reaz et al., 2006]. This model simulates the signal recorded at the skin's surface as a composite signal of the many motor unit action potentials present during voluntary muscle contraction. Randomness is introduced in the MU size, firing frequency, temporal offset and conduction velocity, making the generated signal more lifelike. The model includes type-based recruitment thresholds and firing frequencies, facilitating the simulation of different types of muscle fibres. This allows muscles of differing sizes and compositions to be modelled. The force signal is simulated as a summation of the contributing twitch force trains from each active motor unit.

The results of experimental verification of the model revealed that amplitude characteristics predicted by this model were verified by the experimental data. The spectral properties of simulated signals was shown to have only a small variation with force, which was also similar to experimental results. This sEMG model displays accuracy which may improve the usefulness of sEMG models for research and practical applications.

4.3.4.1 Experimental considerations

For these experiments, 10 second contraction times were used to ensure a gaussian spread of distributed variables in the sEMG model. During 10 second contractions, muscle fatigue did not occur. Neither subject responses or force recordings indicated the presence of muscle fatigue. In each set of experiments, the force output was studied to ensure that variance or unsteadiness of force (indicating increased effort) was not present. If experiments are conducted for longer durations, the possibility of muscle fatigue should be considered. This sEMG model implementation assumes that conduction velocity is constant, so is not suitable for studying fatigued muscles.

For all model validation experiments, the amplitude of the simulated signal was normalised by a factor of κ at the highest contraction level studied (generally 80% MVC). Normalisation is appropriate as the amplitude features of this simulation provide relative, rather than absolute values. This normalisation ensured the magnitude features such as RMS matched closely with the experimental outcome at 80% MVC. The validation experiments investigated whether the rate of change of simulated signal amplitude with contraction strength matched experimental data across all contraction strengths.

4.3.4.2 Amplitude characteristics of the sEMG signal

The sEMG model has inbuilt randomness with simulation parameters following a statistical distribution. When simulated with these distributed variables and non-linear recruitment patterns, the amplitude of the simulated signal was linear with respect to the relative contraction strength (refer to Figure 4.13). The observed linearity of sEMG RMS with %MVC matches the patterns observed experimentally in this work and reported in the literature.

From Table 4.5, it is observed that with the exception of the simulated signals for subject 3, the linear trendlines fit the data well (Table 4.5(b)). The observed rates of change of RMS of sEMG with % MVC (Table 4.5(a)) show that with the exception of subjects 6 and 8, the variation in gradient values is similar between the experimental and simulated results. If the sEMG model is to be considered accurate, then the relationship of the RMS of the simulated sEMG with %MVC should be similar to the experimental result. From Figure 4.12, it is observed that this is correct and that the gradients are quite similar. When considering the average of all participants together (Figure 4.14), the results indicate a close relationship between the simulated and experimental data. A linear relationship is observed in both cases.

4.3.4.3 Frequency characteristics of the sEMG signal

In the verification studies presented, frequency characteristics of the sEMG signal were studied at 30 and 50% MVC. At these contraction levels, there is not expected to be significant changes in the spectrum, as the distribution of motor unit sizes is quite similar. As the experimental duration was 10 seconds, muscle fatigue did not occur, so the conduction velocity of the muscle fibres remained constant. The average firing frequency increases by about 0.5Hz between these two force levels, so will not affect the spectrum greatly.

The number of zero crossings per second did not appear to change with contraction strength. The values calculated for the biceps and the brachioratialis muscles were slightly different from one another. However, the number of zero crossings per second was consistently lower in the simulated data than the acquired experimental data (Tables 4.3 and 4.4). The difference most likely indicates the presence of more noise in the experimental data.

In the model validation work, contraction levels at 30% and 50% MVC were studied. The MNF varied little with either contraction strength or muscle. If contraction levels above 88% MVC were modelled, rate coding theory (increasing firing frequency to increase contraction strength) must be addressed.

The calculated MNFs were consistent with the hypothesis that the frequency would not change significantly at these force levels. Although there was a small increase in the average firing frequency, this was not reflected in the signal features. The lack of variance of MNF and ZC for both the simulated and experimental data sets suggests that changes in firing frequency alone do not have a large impact on the spectrum. Rather, it is likely that changes in the conduction velocity of the muscle fibres will alter the sEMG spectrum, a proposal supported by other researchers [Kleine et al., 2001].

4.3.4.4 Amplitude characteristics of the force signal

The other measurable output of the muscle contraction is the force output. From Figure 4.14, it is observed that both the simulated and experimental force measurements increase at similar rates. As the force output of the model is calculated by the summation of twitch forces from motor units with varying amplitude and time characteristics, the agreement of the simulated force with experimental data serves to validate the model using an alternative method to the comparison between the electrical sEMG signals.

Comparisons of simulated sEMG and force signals with features from experimentally acquired results showed the similarity between the simulated and real muscle data. This model has been validated as providing accurate simulations of skeletal muscle that are not fatigued (time-invariant).

4.4 Conclusion

An sEMG/force model has been implemented and the accuracy of it's simulated signals have been verified against experimental data from healthy adults.

The sEMG/force model incorporates randomness, statistical distributions of parameter values based on experimental data and MU type-based firing frequencies and recruitment patterns to generate sEMG signals that mimic those found in human subjects.

The sEMG signals generated have been shown to be accurate to experimental data by both amplitude and frequency characteristics. The model versatility was verified by simulation of biceps and brachioradialis muscles. Finally, the model was verified by simulation of a force output. The force signal is a summation of the twitch force trains for all active motor units and is influenced by the novel recruitment strategy developed for this work. The force signal was shown to match the output of the force sensor in the experimental work.

As the sEMG/force model has been verified, it can now be used to investigate deviations

from the signals of healthy, young adults. One of the chief uses of modelling is to allow internal process characteristics to be estimated by adapting the model's parameters to reproduce experimental results [Stegeman et al., 2000]. In Chapters 5 and 6, this technique applied as the sEMG/force model is used to study neuromuscular changes with age.

Chapter 5

Model and experiments for neuromuscular changes with age

5.1 Introduction

This chapter describes experiments and simulations conducted to quantify neuromuscular changes with age using the novel sEMG/force model described in Chapters 3 and 4. This work contributes to the understanding of how fast and slow muscle fibre populations change with age. The use of the sEMG/force model to simulate muscles with altered physiology as compared to the muscles of healthy, young adults is demonstrated.

Senescent reduction in muscle mass begins in the third decade of life, but reaches functional significance as people enter their 60s. At this age, the following changes have been observed in skeletal muscles [Moritani et al., 2004] [Bazzucchi et al., 2005]:

- A loss of muscle size
- A loss of maximum force
- No loss of endurance or fatigue resistance

Literature suggests that the loss of muscle force and size is due to;

- A reduction in the total number of muscle fibres
- A reduction in the size of the fibres [Ahad et al., 2005]
- A preferential decrease of type II muscle fibres [Medina, 1996]

Certain exercises can slow the decrease of muscle strength with age [Rogers and Evans, 1993]. Availability of suitable facilities and exercise regimes to assist the ageing population would be beneficial. To allow early intervention, and promote understanding of the movement mechanics of the young-old, it is crucial that these neuromuscular changes are studied.

Anatomical muscle changes with age are reflected in the sEMG signal acquired from a contracting muscle. In this study, sEMG signals were recorded from the bicep muscles of subjects in their 20s and their 60s. The sEMG model described in Chapters 3 and 4 was simulated to generate signals with varying ratios of slow and fast fibre types. The simulated signals and their corresponding fibre type ratios were used to quantify the muscle fibre changes during the ageing process.

5.2 Background

18.6% of the Australian population is over 60 years of age. The ageing of the baby boomers generation has resulted in the largest ever population aged between 60 and 75. This proportion is increasing steadily [ABS, 2009]; by 2020, the proportion of Australians over 65 is predicted to rise by 6% [ABS, 2012].

Recent research has separated the ageing population into two groups, the young-old (60-75 years of age) and the elderly (over 75 years of age). In the young-old group, the neuromuscular system is changing significantly [Cech and Martin, 2012], but the results of the loss of muscle strength such as falls are not as frequent as in the elderly.

Previous research has focused on the muscles of the infirm and elderly, but far fewer studies have investigated changes that occur with young-old subjects [Brown et al., 1988]. While sarcopenia begins in early adulthood, it increases significantly in the sixth decade of life [Cech and Martin, 2012]. This loss of muscle mass is due to a reduction in the number of muscle fibres, particularly of type II muscle fibres [Evans and Lexell, 1995]. A reduction in the size of muscle fibres also contributes to the loss of muscle force with age [Luff, 1998]. However there have been few attempts to quantify these changes.

Current techniques to measure muscle composition either involve intrusive clinical methods such as biopsy [Borg et al., 1987] or rely upon electro-stimulation methods that are both invasive and imprecise [Mc Comas et al., 1993]. These techniques are unsuitable for population-based studies due to the associated pain and inaccuracies. To overcome this limitation, there is an urgent need to develop a reliable, non-invasive methodology for studying muscle composition.

As described in Chapter 2, surface electromyography (sEMG) is non-invasive and easy to record, but does not provided detailed information on individual motor units (MUs). To overcome this limitation, models for sEMG have been developed. One of the chief uses of modelling is to allow internal process characteristics to be estimated by adapting the models parameters to reproduce experimental results [Stegeman et al., 2000].

The model developed and described in Chapters 3 and 4 of this thesis is focused on the simulation of different motor unit types and thus suitable for identifying age-associated changes to the neuromuscular system.

In the experimental work, isometric contractions of the bicep muscle at maximum force were maintained and the sEMG and muscle force outputs were measured. Features of the sEMG signal were compared with features of simulated signals, to determine the physiological changes that have taken place. Statistical analysis of the data sets was conducted.

5.2.1 Surface electromyogram/force model

The use of a physiological model in combination with experimental data provides a method of characterising internal processes or structures from a gross, external signal. Although numerous neuromuscuscular models have been presented, none have sought to accurately simulate the changes in skeletal muscle with age.

To study muscular changes that take place as a result of ageing, a suitable model must use accurate representations of the parameters known to alter. These include

- motor unit firing rates
- motor unit recruitment thresholds
- muscle composition

The sEMG/force model presented and validated in Chapters 3 and 4 of this thesis accurately represents these factors and is thus capable of simulating the whole muscle sEMG and muscle force output signals of the biceps of both younger and older subjects. The neuromuscular model has been previously presented and validated by the author [Wheeler et al., 2010b, Wheeler et al., 2010d, Wheeler et al., 2010e].

This sEMG model differs from models presented by previous authors as it strives to closely align the values and distributions of parameters known to change during disease or ageing with those found in vivo. The model is populated with type-based variables for different motor unit types, allowing slow and fast motor units to be simulated and the effects of the decline in each to be studied.

To predict anatomical changes from the norm using the sEMG model, a set of experimental data is required for comparison with the simulated signals. The experimental methods followed to acquire this data are detailed in Chapter 4 and summarised in the following section.

5.3 Methods

5.3.1 Experimental method

Thirty healthy volunteers participated in this study. All subjects were right-handed and performed the experiments with their dominant hand. The subjects were urban Australians (mixed ethnicity) with no history or symptoms of major muscular, neurological or movement disorders. All participants were moderately active and performed non-strenuous exercise approximately 3-5 times per week. None of the participants were involved in any competitive level sports or engaged in regular rigorous exercise.

Prior to the start of the experiment, the purpose of the study and procedures and risks associated with participation were explained to each subject. Subjects were offered the chance to withdraw from the study at any time. A plain language statement outlining details of the experiments was provided to each participant (Refer to Appendix A), and written informed consent was obtained (Refer to Appendix B). The subjects also filled in an eligibility assessment form which included medical history questions and characteristics including height, weight and bicep circumference (Refer to Appendix C). The experiments were approved by RMIT University Human Research Ethics Committee and were conducted in accordance with the Declaration of Helsinki of 1975, as revised in 2004.

The thirty subjects were divided into two groups:

- Group 1: Younger - 16 subjects; age range 20-28 years
- Group 2: Older - 14 subjects; age range 60-69 years

The laboratory procedures followed to acquire and record sEMG signals from the biceps of human subjects is detailed in Chapter 4. Each subject contracted the bicep to their maximum effort and maintained this contraction for 10 seconds. The subjects were provided with visual feedback of their force output and encouraged to maintain a maximal contraction. Ten seconds

of data was acquired to ensure that muscle fatigue did not occur. During the contractions, both the sEMG and the force outputs were measured.

5.3.2 Data analysis

Post experiment, the signal from the force sensor was viewed to ensure data from a steady contraction was used. The first 5 seconds of data from each subject where the force was held steadily (during the non-fatigued state) was extracted.

To compare signals from the sEMG model with experimental data, a number of signal features were calculated. Each of these features are widely used in the characterisation of sEMG signals and reveal information about the contraction level of the muscle and firing frequency and AP shape of the motor units. Root mean square (RMS) and mean absolute value are related to the amplitude features of the signal. Mean power frequency (MNF) and waveform length describe the frequency distribution of the sEMG. Fractal dimension describes the complexity of the signal.

To eliminate the effects of varying body size and composition, the RMS results were normalised against the body mass index (BMI) of each subject. The BMI is a method of measuring human body fat based on height and weight. Each subject's height and weight were taken from their paperwork and the BMI calculated using equation 5.1.

$$BMI = \frac{mass(kg)}{height(metres)^2} \tag{5.1}$$

The calculated average RMS was then divided by the BMI for each subject.

5.3.3 Simulation method

The sEMG model was used to investigate which neuromuscular changes would yield the age-related signal changes observed experimentally.

To simulate the sEMG/force signals from the biceps muscles of young, healthy adults, the model described in Chapter 3 was simulated with the input parameters listed in Chapter 4. In young, healthy adults, the biceps brachii has a fast fibre ratio (FFR) of approximately 0.45 [Kukulka and Clamann, 1981]. The total number of motor units (nMU) is 110 [Mc Comas et al., 1993], meaning that (varying randomly for each subject) there will be around 50 fast fibre MUs and 60 slow fibre MUs in each young adult bicep muscle.

It is posited that observed neuromuscular changes with age are principally due to a reduction in the number of muscle fibres, particularly fast muscle fibres [Evans and Lexell, 1995, Doherty, 2001]. The nMU and the FFR represent these parameters, so their variance will allow the simulation of signals from older humans.

FFR and nMU were varied to investigate the effect that these parameters have on the RMS and MNF of the generated sEMG signal. Two scenarios were simulated. The first investigated the effect of varying nMU from the values used for a healthy adult (nMU=110). The next studied the effect of varying FFR from the young adult value of 0.45 of MUs.

Literature suggests that the reduction in RMS (and corresponding muscle force) observed in older patients is due to both a drop in the total number of fibres and the size of these remaining fibres. Across the literature, it is generally agreed that the size of type 2 fibres decreases with age, while the size of type 1 fibres remains unchanged [Lexell et al., 1988, Porter et al., 1995, Roos et al., 1997]. Histochemical studies have found that the cross sectional area of type I muscle fibres does not change with age. In work reported by Klein [Klein et al., 2003], the area of type II muscle fibres reduced from 74% to 60% of the total area - a reduction that was not matched by the observed loss of fibre numbers. Klein concluded that with age, a reduction in the largest of the type II muscle fibres occurs. To simulate this phenomenon, the large fibres were preferentially removed from the MU pool when simulating the older adults.

5.4 Results

5.4.1 Experimental results

Table 5.1 shows the mean and standard deviation of six signal features calculated from the older and younger experimental sEMG data sets. In each data set, the subjects were contracting at 100% MVC.

	Experimental subjects	
Feature	Younger	Older
RMS (μV)	7.56 ± 5.45	3.62 ± 1.75
MNF (Hz)	72.84 ± 13.85	77.98 ± 12.32
Complexity	1.162 ± 0.0073	1.143 ± 0.0019
Waveform length	0.083 ± 0.070	0.074 ± 0.074
Mean absolute value	0.15 ± 0.12	0.122 ± 0.11

Table 5.1: Magnitude and spectral averages for older and younger subjects (± value represents the standard deviation)

The results of one-way ANOVA tests to determine the statistical difference of signal features between the older and younger data sets are presented in Table 5.2.

Signal feature	Statistical significance (p value of 1-way ANOVA test)
RMS	0.0117
MNF	0.2551
Complexity	0.0200
Waveform length	0.6980
Mean absolute value	0.4630

Table 5.2: Statistical differences between older and younger subjects

Table 5.2 shows that the difference between the RMS of older and younger subjects is significant, with $p<0.02$. The difference between the MNF of the two groups is not statistically significant, but the mean MNF decreases with age (Table 5.1). Complexity is shown to be statistically different between older and younger subjects, but is known to represent the number of active MUs, which is similarly represented by RMS.

Waveform length and mean absolute value show no statistically significant difference between older and younger subjects, so only RMS and MNF were studied in the remainder of

the work.

5.4.2 Simulation results

Figure 5.1 shows the average RMS and MNF of sEMG signals generated when the number of active motor units was reduced, but the ratio of fast to slow fibres (FFR = 0.45) was maintained. The RMS and MNF at varying nMU values are plotted.

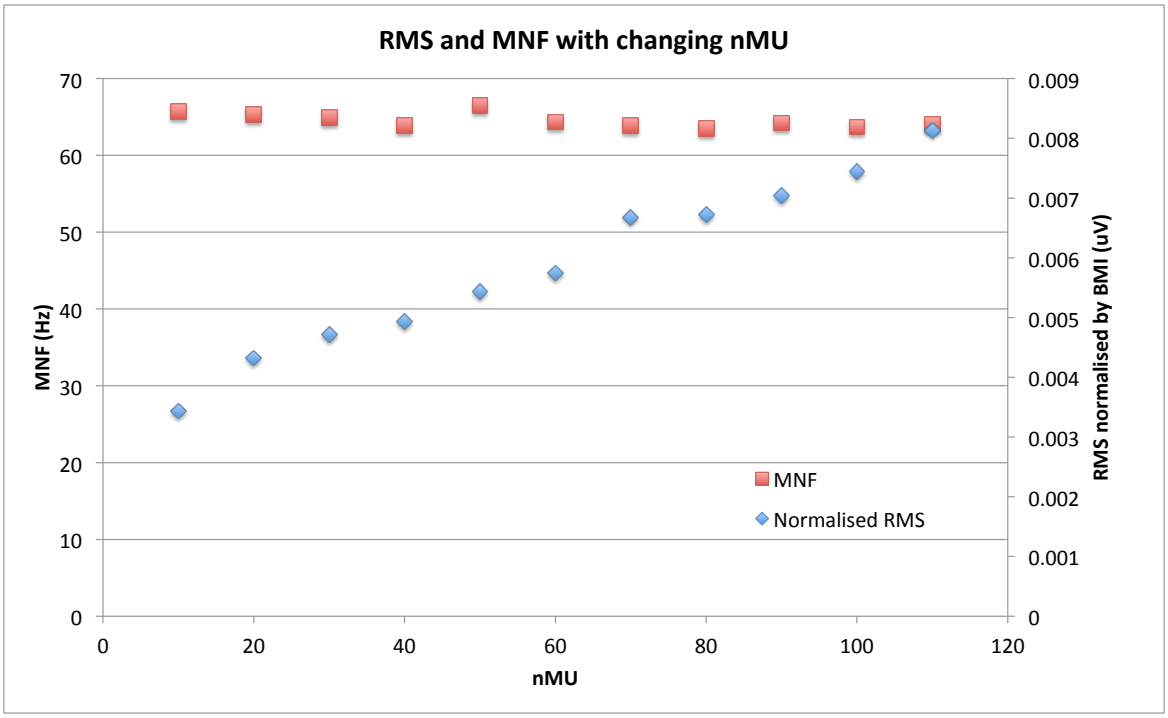

Figure 5.1: RMS and MNF of simulated signals with varying numbers of active motor units

Figure 5.2 shows the results when the number of motor units was kept constant at 110 MU, while the ratio of fast fibres (FFR) was reduced from 0.45 to 0.0 in increments of 0.05. The mean MNF and RMS were plotted against FFR.

In Figure 5.1 and Figure 5.2 it is clear that the number of active motor units affects the RMS of the sEMG signal. The ratio of fast fibres affects both RMS and MNF.

In the experimental data (Table 5.1) the signals from older subjects showed a reduction in

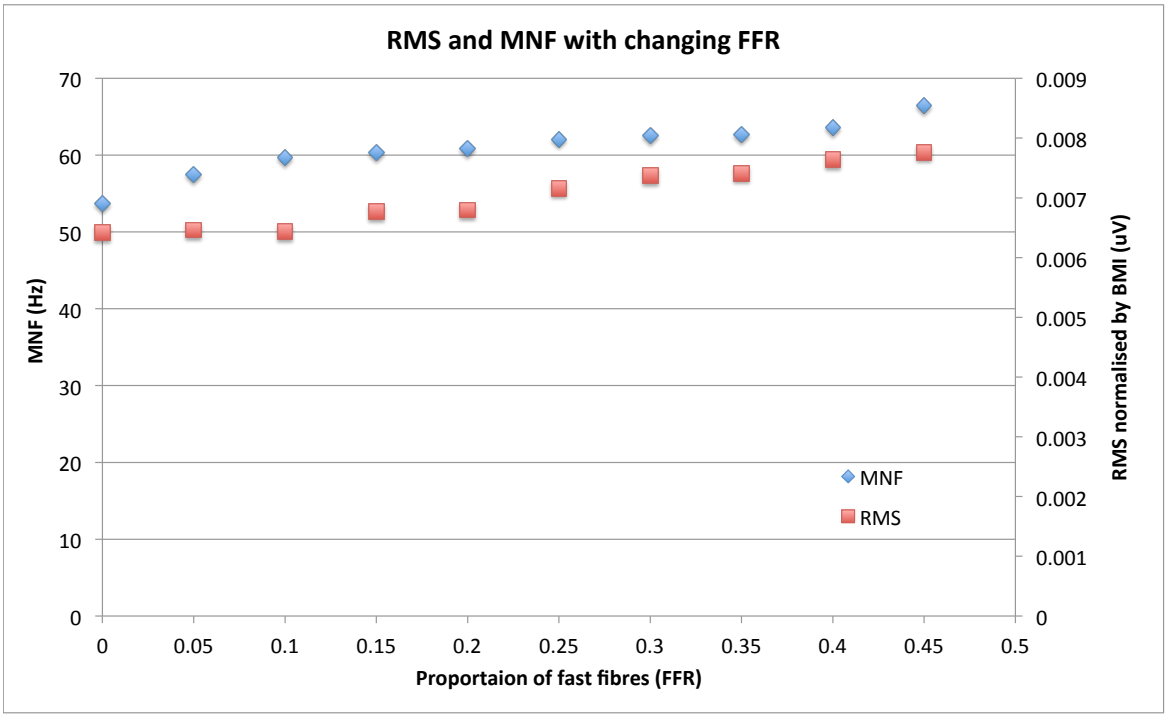

Figure 5.2: MNF and RMS of simulated signals with a varying ratio of fast fibre motor units

mean amplitude of 3.94 mV, and of 5.14 Hz in mean median frequency. To compare simulated and experimental results, sets of simulations were performed with varying input parameters, until the signal features of the generated signals matched those measured from experimental results. Table 5.3 summarises the parameters used to achieve comparable results between simulated and experimental data sets.

	Younger	Older
nMU	110	65
FFR	0.45	0.14

Table 5.3: Simulation parameters used to achieve comparable results between simulated and experimental data

These parameters, in comparison to those used to model a young healthy adult, correspond to an approximate loss of 41 fast fibre MUs and 5 slow fibre MUs. A simulation with these parameters gave an average reduction of 4.16 mV RMS and 5.49 Hz MNF.

5.5 Summary of results

Based on the simulations plotted in Figures 5.1 and 5.2, the input parameters required to generate sEMG signals comparable to the signals recorded from young (subjects in their 20s) and old (subjects in their 60s) have been calculated (Table 5.3). These parameters correspond to an average loss with age of 41 fast fibre MUs and 5 slow fibre MUs.

These fibre losses correspond to the observed effects with age, particularly the maintenance of endurance and the loss of maximal force.

These results, along with the results of validation studies described in Chapter 4, are discussed in detail in Chapter 6: Discussion.

Chapter 6

Discussion

Surface electromyogram modelling is a technique that has been used in a number of research fields. By isolating a single variable to study, researchers have investigated the effects of volume conduction on the sEMG signal [Roeleveld et al., 1997], the influence of electrode size and shape [Farina et al., 2002b] and the separation of motor unit action potential trains from the composite signal [Nakamura et al., 2004].

In this work, an original sEMG model has been implemented. The model has been validated against experimental data recorded from muscles of the human arm. The sEMG model has been used to investigate and quantify muscle composition with age. This is the first time that such a technique has been utilised.

6.1 sEMG/force model

The sEMG/force model implemented in this thesis simulates a lifelike muscle by introducing random elements to give a distribution of parameters, rather than a single value. This variance is seen in real human muscles. Parameters defined by a distribution include the MU size, the firing rate, initial temporal offset and the muscle fibre conduction velocity

[Wheeler et al., 2010b].

Most significantly, this model is populated with distinct features for slow and fast muscle fibre types. This is particularly important when considering muscle changes with age, as fast fibre MU numbers reduce more than slow fibre MU numbers [Wheeler et al., 2010e].

The model includes a type-based motor unit recruitment and firing frequency strategy, in which these parameters are assigned probabilities based on muscle fibre type, so that type I fibres are recruited at low force levels, and type II fibres are recruited with increasing force. Similarly, the firing rate of each motor unit is type based, with firing rates for type I fibres distributed about averages of 8-14 Hz and type II motor units about averages of 12.5 to 24.5 Hz [Wheeler et al., 2010a, Wheeler et al., 2010c].

To ensure that the sEMG model could be accurately validated against experimental data, a second output was added. As well as simulating a sEMG signals, this model simulates the force output of the skeletal muscle contraction [Wheeler et al., 2010d, Wheeler et al., 2011].

6.2 Model validation

This model was validated against data from contracting bicep brachii and brachioradialis muscles. In both cases, the signals were accurate to experimental results, with a signal amplitude that varied linearly with force and a static spectrum in non-fatigued, healthy muscles (Refer to section 4.3)

The results of experimental verification of the model revealed that amplitude characteristics of the simulated signals matched the experimental data. The sEMG model has inbuilt randomness with simulation parameters following a statistical distribution. When simulated with these distributed variables and non-linear recruitment patterns, the amplitude of the simulated signal was linear with respect to the relative contraction strength (refer to Figure 4.13). The observed linearity of sEMG RMS with % MVC matches the patterns observed

experimentally in this work and reported in the literature.

The spectral properties of the simulated signals had only a small variation with force, which was also congruent to experimental results. The sEMG model was shown to display accuracy that could improve the usefulness of sEMG models for research and practical applications.

6.3 Muscular changes with age

The loss of muscle mass with age can be partly accounted for by a reduction in the size of muscle fibres, particularly type II muscle fibres [Evans and Lexell, 1995, Doherty, 2001]. However, the reduction in muscle fibre size is moderate when compared to the overall reductions in muscle mass observed with age. Senescent atrophy appears to be largely due to a reduction in muscle fibre numbers, particularly in type II muscle fibres [Evans and Lexell, 1995].

In the work presented in this paper, the physiological changes that led to the observed reduction in muscle force have been quantified. SEMG data from the biceps muscles of younger and older subjects were acquired and a number of signal features were calculated. The RMS feature was used to represent the force output of the muscle. The MNF signal feature represented the spectral properties of the sEMG.

6.3.1 Changes in the number of motor units

The experimental results indicated a significant age-related reduction in the RMS of the signal. Table 5.1 shows an average RMS of 7.56 uV in younger subjects, and 3.62 uV in older subjects. The ANOVA test (Table 5.2) showed a significant difference in RMS between the two groups, with a P-value of 0.0117.

Simulation studies were used to investigate the factors that contributed to the change in RMS. Figure 5.1 showed that a drop in the total number of fibres (nMU) results in a reduction in RMS. RMS is dependent on nMU in an approximately linear relationship. This indicates

that the experimentally observed reduction in RMS is due to a corresponding reduction in nMU.

A reduction in the number of muscle fibres in the biceps brachii with age is in line with results reported in the literature. Lexell reported that subjects in their 90s had around half the muscle fibres of those in a 20 year old [Lexell et al., 1988]. Brown, Strong and Snow studied the bicep contractions of 40 subjects and found that subjects over 60 years old had around half the motor units of subjects in their 30s [Brown et al., 1988].

Figure 5.2 showed that for simulated results, a change in the FFR with unchanged MU numbers results in a small drop in RMS. This is because the fast fibre motor units are larger in size and produce larger amplitude action potentials. However, the majority of the observed reduction in sEMG RMS with age is due to the reduction in nMU.

6.3.2 Changes in the ratio of fast muscle fibres.

In healthy young people, the bicep muscle comprises of around 45% type II (fast) muscle fibres and 65% type I muscle fibres. The reduction observed in the number of muscle fibres with age is not uniform. Fast fibre numbers have been found to reduce more with age than slow fibre numbers [Lexell et al., 1988, Evans and Lexell, 1995].

This work sought to quantify the ratio of fast and slow fibres in young-old subjects as compared to the young. The MNF was used to represent the composition of fast and slow motor units in the muscle. As the firing frequencies of slow fibres are lower than the firing frequencies of fast fibres, the mean power frequency (MNF) depends upon the ratio of these fibre types in the muscle. Analysis of the experimental sEMG of young and old subjects showed that the average MNF reduced with age from 78-72 Hz. From Figure 5.1, it was evident that in the simulation study, the number of MUs did not have a significant impact on the sEMG spectrum.

Figure 5.2 showed that when the ratio of fast fibres (FFR) was changed, there was an

observable change in median frequency. A reduction in FFR from 0.45 showed a related reduction in MNF.

6.3.3 A combined model of muscular changes with age

Based on the simulations plotted in Figures 5.1 and 5.2, the input parameters required to generate sEMG signals comparable to the experimental data were calculated (Table 5.3). These parameters, in comparison to those used to model a younger subject, correspond to an approximate loss of 41 fast fibre MUs and 5 slow fibre MUs. These fibre losses correspond to the observed effects with age, particularly the maintenance of endurance and the loss of maximal force.

A simulation with these parameters gave a mean MNF drop of 5.49 Hz, and a mean RMS reduction of 4.16 mV, which correspond closely to the age-related changes observed in the experimental data (Table 6.1).

	Experimental	Simulated
RMS	3.93 mV	4.16 mV
MNF	5.14 Hz	5.49 Hz

Table 6.1: Changes in sEMG signal features between younger and older subjects

6.4 Model assumptions

As with all biological models, the model presented in this work makes some assumptions to allow rapid and repeatable signals to be generated. Chief among these is the muscle shape, which is simulated as a cylinder, rather than the fusiform shape which is typical of a bicep muscle (refer to Figure 3.4). This has limited impact on the composite signal, as the muscle fibres in a biceps muscle are approximately parallel.

In addition, the modelling of each motor unit as a scaled single fibre is an approximation. To account for the effects of volume conduction more accurately, the fibres in a motor unit

should be simulated as distributed throughout a territory.

Further assumptions that could be eliminated in future work include time invariance (which limits the simulation capability to non-fatigued muscles), single-layer cutaneous tissue and uniform muscle fibre length.

6.5 Experimental limitations

An experimental limitation of this work concerns the contributions of all four muscles to the flexion of the elbow. As the contribution of each muscle can not be determined via sEMG, it can not be assumed that increases in force vary linearly with increases in the contraction strength of any given muscle.

Future experimentalists could also consider offsetting electrode placement from measured innervation zones (to increase the comparability of results between subjects) and the advantages to be gained from a higher resolution of electrodes.

Chapter 7

Conclusions

7.1 Ageing conclusions

Subjects in their sixth decade show a loss of 41% of the motor units in the biceps brachii muscle, with a preferential loss of fast fibre motor units. The ratio of fast fibre motor units to slow fibre motor units reduces from 0.45 observed in subjects in their 20s, to 0.14 for subjects in their 60s.

Of the 14 older subjects studied in this work, a reduction in average sEMG RMS of 52% and a reduction in average sEMG MNF of 5.14 Hz were observed.

A sEMG model with lifelike simulation parameters was used to simulate sEMG signals from younger and older subjects. The spectral shift in sEMG signals observed in the bicep contractions of older subjects was shown to match the experimental data when the ratio of fast fibres was reduced from 0.45 to 0.14 and the total number of fibres was dropped from 110 to 65. When the larger MU were preferentially removed from the pool, these same simulating conditions were shown to account for the observed drop in signal RMS.

7.2 Response to research questions

As outlined in section 1.3, the work in this thesis attempted to answer the following research questions;

- How does the neuromuscular system change with age?
- Specifically, do different muscle fibre types react the same way to the ageing process?
- Can a sEMG/force model be used to quantify such changes?

Through the implementation of a novel, versatile and robust sEMG/force model, these research questions have been answered. The extent to which the neuromuscular system changes with age have been studied and quantified in Chapters 5 and 6. By simulating a variety of different muscle contraction scenarios, and comparing the signal with experimental results, it is concluded that the different muscle types do not react the same way to the ageing process. The experimental work presented here agrees with current literature which proposes that fast muscle fibre types reduce in number more rapidly with age than slow muscle fibres.

This work has shown that an appropriately designed and implemented sEMG/force model can be used to quantify muscular changes from the norm, such as those detected in ageing adults. In the future, this model could be used to study alternate physiology such as injured, diseased or fatigued human muscles.

Appendix A

Plain language statement for participants

RMIT UNIVERSITY

School of Electrical & Computer Engineering

Project information statement

1. Project title

Electromyogram features for muscle fatigue assessment and muscle changes with age

2. Investigators

- Ms Katherine Wheeler, PhD candidate, School of Electrical and Computer Engineering, RMIT University.
Ph: 9925 5234 Email: s3221776@student.rmit.edu.au
- Dr Sridhar P Arjunan, Research Associate, School of Electrical and Computer Engineering, RMIT University
Ph: 9925 5234 Email: sridhar.arjunan@rmit.edu.au
- Dr Dinesh K Kumar, Professor, School of Electrical and Computer Engineering, RMIT University
Ph: 99251954 Email: dinesh@rmit.edu.au
- Ms Savithry Thangaraju, 03 9925 3781, School of Electrical and Computer Engineering, RMIT University. Email: savithry.thangaraju@student.rmit.edu.au

3. Who is involved in this project?

This project is currently being conducted by RMIT University, in the School of Electrical and Computer Engineering. This project has no external or commercial partners. This project has been approved by the RMIT Human Research Ethics Committee and RMIT Science Engineering and Technology Portfolio Higher Degree by Research Committee.

Why are these experiments being conducted?:

18.6% of the Australian population is over 60 years of age and this proportion is increasing steadily [ABS, 2009]. A normal part of the ageing process includes neuromuscular changes that can affect steadiness and strength. As these changes affect such a large proportion of the population, it is crucial that the underlying mechanisms behind these neuromuscular changes are understood.

To understand these changes, we are recording bicep muscle signals from healthy participants ranging in age from 20-80 years old. These signals will be compared with a mathematical model of the bicep muscle so that changes with age can be calculated.

This knowledge may allow early intervention of muscular weakness and improved protocols for maintaining strength with age.

If I agree to participate, what will I be asked to do?:

From these experiments, we require recordings of muscle signals from both fatigued and non-fatigued muscles. The majority of experiments will be conducted on the muscles of the upper arm. You will therefore be asked to hold bicep muscle flexion at different forces for short periods.

We will record your muscle signals the entire time, but are especially interested in the signals at the beginning of the recording (when the muscles are fresh) and at the end of the experiment (when the muscles are getting tired).

There will be plenty of rest time between each contraction.

We will be recording from muscles in the upper arms, using electrodes (metal disks) that are attached to the surface of your skin with adhesive, similar to a bandaid. If you are also involved in the experiments on the lower limbs, these same electrodes will be affixed to the skin surface above the quadriceps muscles of the thigh. Before the electrodes are attached, you skin will be exfoliated and cleaned with an alcohol wipe. Your skin will be shaved (with your permission) if required, but this is rarely the case. Between 4 and 8 electrodes will be attached. These electrodes will allow us to record the electrical activity in your muscles, below the electrode site. The electrodes will not cause you any pain or discomfort. If you feel discomfort as they are removed (similar to removing a bandaid), you may advise the investigator and they will offer you moisturising lotion to soothe the site.

What are the benefits associated with my participation?

There are no direct benefits to you for your participation. However, your participation will be helpful in conducting this research, which may lead to improvements in the treatment of neuromuscular complaints.

What are the risks associated with my participation?

There are no perceived risks outside your' normal day-to-day activities associated with participation in this research project. The hair from the electrode site may be shaven (if necessary) before placement of electrodes using common razors. Some participants may experience some mild discomfort during the removal of the electrodes due to the adhesive. This is not common and is very mild in the worst case. We could provide you with moisturiser if it is required. If you experience any discomfort, then proper on-site care will be provided by the University Health Services located in Building 14, level 4 (ph: 9925 2078). After holding the muscle contractions for a minute, you may experience muscle soreness post experiment, similar to that experienced after mild exercise. If you are participating in experiments on the lower limbs, you will be asked to wear shorts on the day.

What will happen to the information I provide?

The muscle activity data collected from you will be stored on a computer for analysis and will also be kept in a locked file cabinet in the biosignal lab on 10.7. Only the project investigators will have access to the computer and the cabinet. You will not be identifiable from your muscle activity data.
Any information that you provide can be disclosed only if
(1) it is to protect you or others from harm,
(2) a court order is produced, or
(3) you provide the researchers with written permission
Results from the muscle activity data will be reported in the project report. These results may also be published in technical journals and conference papers. Your identity will NOT be disclosed in any form in any of the publications of this project. The research data will be kept securely at RMIT for a period of 5 years before being destroyed.

What are my rights as a participant?

As a participant of this research project, you have the right to withdraw your participation at any time, without prejudice. You also have the right to have any unprocessed data withdrawn and destroyed, provided it can be reliably identified and provided that doing so does not increase the risk for you. You have the right to have any questions relevant to the experiment answered at any time.

Whom should I contact if I have any questions?

If you have any queries regarding this research, you can contact:
Katherine Wheeler: 03 9925 5234, email s3221776@student.rmit.edu.au
Dr. Sridhar Poosapadi Arjunan: 03 9925 5234, email sridhar.arjunan@rmit.edu.au
Professor Dinesh Kant Kumar (PhD): 03 9925 1954, email dinesh@rmit.edu.au
Ms Savithry Thangaraju, 03 9925 3781, savithry.thangaraju@student.rmit.edu.au

What other issues should I be aware of before deciding whether to participate?

The experiments are for people in the age group of 18 to 80 who do not have any known neuromuscular health ailments. You should not be in any dependent relationship with any of the investigators. If you are a student of the investigator on this project, please advise us.

Yours Sincerely

K Wheeler	S P Arjunan	D K Kumar	J. Gubbi	C Kalra	S Thangaraju
(M.Engg) B.Eng	(PhD) M.Engg	PhD, B.Eng.	PhD., B. Eng	B.E. M.E.	B.E. M.E.

Any complaints about your participation in this project may be directed to the Secretary, RMIT Human Research Ethics Committee, University Secretariat, RMIT, GPO Box 2476V, Melbourne, 3001. The telephone number is (03) 9925 1745.
Details of the complaints procedure are available from the above address.

Appendix B

Informed consent

Prescribed Consent Form For Persons Participating In Research Projects Involving Tests and/or Medical Procedures

Portfolio		**Science, Engineering and Technology**		
School of		**Electrical and Computer Engineering**		
Name of participant:				
Project Title:		Electromyogram features for muscle fatigue assessment		
Name(s) of investigators:	(1)	**Katherine Wheeler**	Phone:	**992 54805**
	(2)	**A/Prof. Dinesh Kant Kumar**	Phone:	**992 51954**
	(3)	**Sridhar Arjunan**	Phone:	**992 54805**
	(4)	**Dr Jayavardhana Gubbi**	Phone:	**834 48146**

1. I have received a statement explaining the tests/procedures involved in this project.

2. I consent to participate in the above project, the particulars of which - including details of tests or procedures - have been explained to me.

3. I authorise the investigator or his or her assistant to use with me the tests or procedures referred to in 1 above.

4. I acknowledge that:

   (a) The possible effects of the tests or procedures have been explained to me to my satisfaction.
   (b) I have been informed that I am free to withdraw from the project at any time and to withdraw any unprocessed data previously supplied (unless follow-up is needed for safety).
   (c) The project is for the purpose of research and/or teaching. It may not be of direct benefit to me.
   (d) The privacy of the personal information I provide will be safeguarded and only disclosed where I have consented to the disclosure or as required by law.
   (e) The security of the research data is assured during and after completion of the study. The data collected during the study may be published, and a report of the project outcomes will be provided to **RMIT University, HDRC, SECE, and ARC**. Any information which will identify me will not be used.

Participant's Consent

Participant: _____ **Date:** _____
(Signature)

Witness: _____ **Date:** _____
(Signature)

Participants should be given a photocopy of this consent form after it has been signed.

Any complaints about your participation in this project may be directed to the Executive Officer, RMIT Human Research Ethics Committee, Research & Innovation, RMIT, GPO Box 2476V, Melbourne, 3001. The telephone number is (03) 9925 2251. Details of the complaints procedure are available from the above address.

.

Appendix C

Eligibility assessment form

RMIT UNIVERSITY

School of Electrical & Computer Engineering

Eligibility assessment and general health information

1. Project title

Electromyogram features for muscle fatigue assessment

2. Investigators

- Ms Katherine Wheeler, PhD candidate, School of Electrical and Computer Engineering, RMIT University.
Ph: 99254805 Email: s3221776@student.rmit.edu.au
- Mr Sridhar P Arjunan, Research Associate, School of Electrical and Computer Engineering, RMIT University
Ph: 99254805 Email: s3099587@student.rmit.edu.au
- Dr Dinesh K Kumar, Associate Professor, School of Electrical and Computer Engineering, RMIT University
Ph: 99251954 Email: dinesh@rmit.edu.au
- Dr Jayavardhana Gubbi, Research fellow, Biomedical Signal Processing, The University of Melbourne
Ph: 834 48146 Email: jgl@unimelb.edu.au

3. Letter of explanation and information recording

Dear participant,

Thankyou for agreeing to participate in the experiment *Electromyogram features for muscle fatigue assessment* at RMIT University. For information on what is required during the experiment, please refer to the project information statement provided by the investigator.

Please provide the following general information;

Name: _____

Date of birth: _____

Gender (M/F): _____

Height: _____

Weight: _____

Dominant hand _____

Hand used for experiment _____

Bicep circumference (unflexed) _____

Bicep circumference (flexed) _____

In order to participate in this experiment, there are a number of criteria which must be met. In order to allow the investigator to assess your eligibility, please complete the following checklist;

1. Are you a student of the chief investigator (Katherine Wheeler) Yes ☐ No ☐

2. Are you a student of one of the other investigators? Yes ☐ No ☐

3. Do you suffer from arthritis (i.e. osteoarthritis or rheumatoid arthritis)? Yes ☐ No ☐

4. Do you suffer from a neuromuscular disorder? Yes ☐ No ☐

5a. Have you ever injured your wrist or hand? Yes ☐ No ☐

5b. If so, please describe the injury and give a date of the injury

Description:

_____

_____

_____

Date: _____

6. Do you have any other conditions (medical or otherwise) which you think may exclude you from this project?

Yes ☐ No ☐

If so, please provide details:

_____

_____

_____

4. Process

Thankyou for filling out this eligibility form. If you have answered “yes” to any of the questions above, the investigator will discuss your answers with you to determine your eligibility.

_____ _____

Katherine Wheeler
(M.Eng) B.Eng

Date

_____ _____

Other investigator

Date

Eligibility notes:

Any complaints about your participation in this project may be directed to the Secretary, RMIT Human Research Ethics Committee, University Secretariat, RMIT, GPO Box 2476V, Melbourne, 3001. The telephone number is (03) 9925 1745.
Details of the complaints procedure are available from the above address.

Bibliography

[ABS, 2009] ABS (2009). Disability, ageing and carers, australia: Summary of findings. Technical report, Australian Bureau of Statistics.

[ABS, 2012] ABS (2012). Year book of australia, 2012. Technical report, Australian Bureau of Statistics.

[Ahad et al., 2005] Ahad, M. A., Wertsch, J. J., and Ferdjallah, M. (2005). Analysis of computer generated muscle action potentials during simulated aging process. In *Circuits and Systems*, page 1774.

[Arabadzheiv et al., 2010] Arabadzheiv, T. I., Dimitrov, G. V., Dimitrova, N. A., and Dimitrov, V. G. (2010). Influence of motor unit synchronization on amplitude characteristics of surface and intramuscularly recorded emg signals. *European Journal of Applied Physiology*, 108(2):227–237.

[Arjunan and Kumar, 2007] Arjunan, S. and Kumar, D. (2007). Fractal based modelling and analysis of electromyography (emg) to identify subtle actions. In *Engineering in Medicine and Biology Society, 2007. EMBS 2007. 29th Annual International Conference of the IEEE*, pages 1961–1964. TY - CONF.

[Basmajian, 1978] Basmajian, J. (1978). *Muscles Alive: Their Functions Revealed by Electromyography*. The Williams and Wilkins Company, Baltimore, fourth edition.

[Bazzucchi et al., 2005] Bazzucchi, I., Marchetti, M., Rosponi, A., Fattorini, L., Castellano, V., Sbriccoli, P., and Felici, F. (2005). Differences in the force/endurance relationship between young and older men. *European Journal of Applied Physiology*, 93:390–397.

[Blok et al., 2002] Blok, J., Stegeman, D., and Van Oosterom, A. (2002). Three-layer volume conductor model and software package for applications in surface electromyography. *Annals of biomedical engineering*, 30:566–577.

[Borg et al., 1987] Borg, J., Edstrom, L., Butler-Brown, G., and Thornell, L.-E. (1987). Muscle fibre type composition, motoneuron firing properties, axonal conduction velocity and refractory period for foot extensor motor units in dystrophia myotonica. *Journal of Neurology, Neurosurgery and Psychiatry*, 50:1036–1044.

[Bowden and Bowden, 2002] Bowden, B. and Bowden, J. (2002). *An illustrated atlas of skeletal muscles*. 2nd edition.

[Brown et al., 1988] Brown, W., Strong, M., and Snow, R. (1988). Methods for estimating numbers of motor units in biceps-brachialis muscles and losses of motor units with aging. *Muscle and Nerve*, 11(5):423–432. 10.1002/mus.880110503.

[Calder et al., 2008] Calder, K. M., Stashuk, D. W., and McLean, L. (2008). Physiological characteristics of motor units in the brachioradialis muscle across fatiguing low-level isometric contractions. *Journal of Electromyography and Kinesiology*, 18(1):2–15.

[Cech and Martin, 2012] Cech, D. and Martin, S. (2012). *Functional movement development across the lifespan*. Saunders, St Louis.

[Christakos, 1982] Christakos, C. N. (1982). A study of the electromyogram using a population stochastic model of skeletal muscle. *Biological Cybernetics*, 45(1):5–12.

[Cooper, 2000] Cooper, G. (2000). *The cell: A molecular approach*, volume 1. ASM Press, Washington DC, second edition.

[Cram et al., 1998] Cram, J., Kasman, G., and Holtz, J. (1998). *Introduction to Surface Electromyography*. Aspen Publishers, Michigan.

[DeLuca, 1975] DeLuca, C. J. (1975). A model for a motor unit train recorded during constant force isometric contractions. *Biological Cybernetics*, 19(3):159–167.

[DeLuca and Hostage, 2010] DeLuca, C. J. and Hostage, E. (2010). Relationship between firing rate and recruitment threshold of motoneurons in voluntary isometric contractions. *Journal of Neurophysiology*, 104:1034–1046.

[Doherty, 2001] Doherty, T. J. (2001). The influence of aging and sex on skeletal muscle mass and strength [review]. *Current Opinion in Clinical Nutrition and Metabolic Care*, 4(6):503–508.

[Duchene and Hogrel, 2000] Duchene, J. and Hogrel, J. (2000). A model of emg generation. *IEEE Transactions on Biomedical Engineering*, 47(2):192–201.

[Dumitru et al., 1999] Dumitru, D., King, J., and Rogers, W. (1999). Motor unit action potential components and physiologic duration. *Muscle and Nerve*, 22(6):733–741.

[Evans and Lexell, 1995] Evans, W. J. and Lexell, J. (1995). Human aging, muscle mass, and fiber type composition. *The Journals of Gerontology Series A: Biological Sciences and Medical Sciences*, 50A(Special Issue):11–16.

[Farina et al., 2002a] Farina, D., Cescon, C., and Merletti, R. (2002a). Influence of anatomical, physical, and detection-system parameters on surface emg. *Biological Cybernetics*, 86(6):445–456. 10.1007/s00422-002-0309-2.

[Farina and Enoka, 2011] Farina, D. and Enoka, R. M. (2011). Surface emg decomposition requires an appropriate validation. *The American Physiological Society*, 105(2):981–982.

[Farina et al., 2002b] Farina, D., Fattorini, L., Felici, F., and Filligoi, G. (2002b). Nonlinear surface emg analysis to detect changes of motor unit conduction velocity and synchronization. *J Appl Physiol*, 93(5):1753–1763.

[Farina et al., 2004] Farina, D., Merletti, R., and Enoka, R. M. (2004). The extraction of neural strategies from the surface emg. *J Appl Physiol*, 96(4):1486–1495.

[Fuglevand et al., 1993] Fuglevand, A. J., Winter, D. A., and Patla, A. E. (1993). Models of recruitment and rate coding organization in motor-unit pools. *J Neurophysiol*, 70(6):2470–2488.

[Gray, 1973] Gray, H. (1973). *Gray's Anatomy*. Longman, London, 35 edition.

[Gydikov and Kosarov, 1974] Gydikov, A. and Kosarov, D. (1974). Some features of different motor units in human biceps brachii. *Pflgers Archiv European Journal of Physiology*, 347(1):75–88. 10.1007/BF00587056.

[Hamilton-Wright and Stashuk, 2005] Hamilton-Wright, A. and Stashuk, D. W. (2005). Physiologically based simulation of clinical emg signals. *Biomedical Engineering, IEEE Transactions on*, 52(2):171–183.

[Jennett, 1989] Jennett, S. (1989). *Human Physiology*. Churchill Livingstone, Edinburgh.

[Johansson, 2005] Johansson, C. (2005). Biceps.

[Kandell et al., 2000] Kandell, E., Schwartz, J., and Jessell, T. (2000). *Principles of Neural Science*. New York, fourth edition edition.

[Klein et al., 2003] Klein, C. S., Marsh, G. D., Petralla, R. J., and Rice, C. L. (2003). Muscle fiber number in the biceps brachii muscle of young and old men. *Muscle and Nerve*, 28(1):62.

[Kleine et al., 2001] Kleine, B. U., Stegeman, D. F., Mund, D., and Anders, C. (2001). Influence of motoneuron firing synchronization on semg characteristics in dependence of electrode position. *J Appl Physiol*, 91(4):1588–1599.

[Krogh-Lund and Jrgensen, 1992] Krogh-Lund, C. and Jrgensen, K. (1992). Modification of myo-electric power spectrum in fatigue from 15maximal voluntary contraction of human elbow flexor muscles, to limit of endurance: reflection of conduction velocity variation

and/or centrally mediated mechanisms? *European Journal of Applied Physiology and Occupational Physiology*, 64(4):359–370.

[Kukulka and Clamann, 1981] Kukulka, C. G. and Clamann, H. P. (1981). Comparison of the recruitment and discharge properties of motor units in human brachial biceps and adductor pollicis during isometric contractions. *Brain Research*, 219(1):45–55.

[Lexell et al., 1988] Lexell, J., Taylor, C., and Sjostrom, M. (1988). What is the cause of the ageing atrophy? total number, size and proportion of different fiber types studied in whole vastus lateralis muscle from 15- to 83-year-old men. *Journal of Neurological Science*, 84(2-3):275–94.

[Lo Conte and Merletti, 1995] Lo Conte, L. R. and Merletti, R. (1995). Advances in signal processing of surface myoelectric signals. part 2. *Medical and Biological Engineering and Computing*, 33:372–384.

[Loeb and Gans, 1986] Loeb, G. and Gans, C. (1986). *Electromyography for Experimentalists*. The University of Chicago Press, Chicago, first edition.

[Lowery et al., 2000] Lowery, M. M., Vaughan, C. L., Nolan, P. J., and O'Malley, M. J. (2000). Spectral compression of the electromyographic signal due to decreasing muscle fiber conduction velocity. *Rehabilitation Engineering, IEEE Transactions on*, 8(3):353–361.

[Luff, 1998] Luff, A. R. (1998). Age-associated changes in the innervation of muscle fibers and changes in the mechanical properties of motor units. *Annals of the New York Academy of Sciences*, 854(1):92–101.

[Martini, 2004] Martini, F. (2004). *Fundamentals of Anatomy and Physiology*. Prentice Hall, San Francisco, CA, sixth edition.

[Mc Comas et al., 1993] Mc Comas, A., J., Galea, V., and de Bruin, H. (1993). Motor unit populations in healthy and diseased muscles. *Physical Therapy*, 73(12):868–877.

[Medina, 1996] Medina, J. J. (1996). *The Clock of Ages*. Cambridge University Press, Cambridge.

[Merletti et al., 2008] Merletti, R., Holobar, A., and Farina, D. (2008). Analysis of motor units with high-density surface electromyography. *Journal of Electromyography and Kinesiology*, 18(6):879–890. doi: DOI: 10.1016/j.jelekin.2008.09.002.

[Merletti et al., 1999a] Merletti, R., Lo Conte, L., Avignone, E., and Guglielminotti, P. (1999a). Modeling of surface myoelectric signals. i. model implementation. *Biomedical Engineering, IEEE Transactions on*, 46(7):810–820.

[Merletti and Lo Conte, 1995] Merletti, R. and Lo Conte, L. R. (1995). Advances in signal processing of surface myoelectric signals. part 1. *Medical and Biological Engineering and Computing*, 33:362–372.

[Merletti et al., 1999b] Merletti, R., Roy, S. H., Kupa, E., Roatta, S., and Granata, A. (1999b). Modeling of surface myoelectric signals. ii. model-based signal interpretation. *Biomedical Engineering, IEEE Transactions on*, 46(7):821–829.

[Mesin et al., 2009] Mesin, L., Merletti, R., and Rainoldi, A. (2009). Surface emg: The issue of electrode location. *Journal of Electromyography and Kinesiology*, 19(5):719–726. doi: DOI: 10.1016/j.jelekin.2008.07.006.

[Mesin et al., 2011] Mesin, L., Merletti, R., and Vieira, T. M. M. (2011). Insights gained into the interpretation of surface electromyograms from the gastrocnemius muscles: A simulation study. *Journal of Biomechanics*, 44(6):1096–1103.

[Moritani et al., 2004] Moritani, T., Stegeman, D., and Merletti, R. (2004). *Basic Physiology and Biophysics of EMG Signal Generation*. IEEE.

[Nakamura et al., 2004] Nakamura, H., Yoshida, M., Kotani, M., Akazawa, K., and Moritani, T. (2004). The application of independent component analysis to the multi-channel surface

electromyographic signals for separation of motor unit action potential trains: part i–measuring techniques. *Journal of Electromyography and Kinesiology*, 14(4):423–432. 1050-6411 doi: DOI: 10.1016/j.jelekin.2004.01.004.

[Oskoei and Huosheng, 2008] Oskoei, M. A. and Huosheng, H. (2008). Support vector machine-based classification scheme for myoelectric control applied to upper limb. *Biomedical Engineering, IEEE Transactions on*, 55(8):1956–1965.

[Pan et al., 1989] Pan, Z., Zhang, Y., and Parker, P. (1989). Motor unit power spectrum and firing rate. *Medical and Biological Engineering and Computing*, 27(1):14–18.

[Plonsey, 1974] Plonsey, R. (1974). The active fiber in a volume conductor. *Biomedical Engineering, IEEE Transactions on*, BME-21(5):371–381. EMG model: Describes how the porential generated by the fiber is expressed at the surface.

[Porter et al., 1995] Porter, M. M., Vandervoort, A. A., and Lexell, J. (1995). Aging of human muscle: structure, function and adaptability. *Scandinavian Journal of Medicine and Science in Sports*, 5(3):129–142.

[Reaz et al., 2006] Reaz, M., Hussain, M., and Mohd-Yasin, F. (2006). Techniques of emg signal analysis: detection, processing, classification and applications. *Biological Procedures Online*, 8(1):11–35. 10.1251/bpo115.

[Roeleveld et al., 1997] Roeleveld, K., Blok, J. H., Stegeman, D. F., and van Oosterom, A. (1997). Volume conduction models for surface emg; confrontation with measurements. *Journal of Electromyography and Kinesiology*, 7(4):221–232.

[Rogers and Evans, 1993] Rogers, M. A. and Evans, W. J. (1993). Changes in skeletal muscle with aging: effects of exercise training. *Exercise and sport sciences reviews*, 21:65–102. Review.

[Roos et al., 1997] Roos, M. R., Rice, C. L., and Vandervoort, A. A. (1997). Age-related changes in motor unit function. *Muscle and Nerve*, 20(6):679–690.

[Rosenfalck, 1969] Rosenfalck, P. (1969). Intra and extra-cellular potential fields of active nerve and muscle fibres. *Acta Physiologica Scandinavica*, Supplementum 321:1–166.

[Seniam, 2009] Seniam (2009). Surface electromyography for the non-invasive assessment of muscles.

[Stashuk, 1993] Stashuk, D. W. (1993). Simulation of electromyographic signals. *Journal of Electromyography and Kinesiology*, 3(3):157–173.

[Stegeman et al., 2000] Stegeman, D. F., Blok, J. H., Hermens, H. J., and Roeleveld, K. (2000). Surface emg models: properties and applications. *Journal of Electromyography and Kinesiology*, 10(5):313–326. doi: DOI: 10.1016/S1050-6411(00)00023-7.

[Stegeman et al., 2004] Stegeman, D. F., Merletti, R., and Hermens, H. J. (2004). *EMG modelling and simulation*, pages 205 – 232. Institute for Electrical and Electronic Engineers.

[Tenore, 2007] Tenore, F. (2007). Towards the control of individual fingers of a prosthetic hand using surface emg signals. In *Engineering in Medicine and Biology Society, 2007. 29th Annual International Conference of the IEEE*, pages 6145 – 6148. IEEE.

[van Veen et al., 1993] van Veen, B. K., Wolters, H., Wallinga, W., Rutten, W. L., and Boom, H. B. (1993). The bioelectrical source in computing single muscle fiber action potentials. *Biophysical Journal*, 64(5):1492–1498.

[Wakeling, 2009] Wakeling, J. M. (2009). Patterns of motor recruitment can be determined using surface emg. *Journal of Electromyography and Kinesiology*, 19(2):199–207.

[Wheeler et al., 2010a] Wheeler, K., Kumar, D. K., and Shimada, H. (2010a). Changing motor unit firing frequencies with force in the human biceps brachii. In *Biosignals 2010*, volume 20 of *Analysis of Biomedical Signals and Images*, pages 425–430.

[Wheeler et al., 2010b] Wheeler, K., Shimada, H., and Kumar, D. K. (2010b). An adaptable model for simulating whole muscle surface electromyogram. In *ISSNIP Biosignals and Biorobotics Conference*.

[Wheeler et al., 2010c] Wheeler, K., Shimada, H., and Kumar, D. K. (2010c). A whole muscle semg model with an accurate recruitment stragegy.

[Wheeler et al., 2010d] Wheeler, K. A., Kumar, D. K., and Shimada, H. (2010d). An accurate bicep muscle model with semg and muscle force outputs. *Journal of Medical and Biological Engineering*, 30(6):393–399.

[Wheeler et al., 2011] Wheeler, K. A., Kumar, D. K., Shimada, H., and Weghorn, H. (2011). Implementing a surface emg model with accurate parameters and a force output. *ISSNIP Biosignals and Biorobotics Conference*.

[Wheeler et al., 2010e] Wheeler, K. A., Shimada, H., Kumar, D. K., and Arjunan, S. P. (2010e). A semg model with experimentally based simulation parameters. In *32nd Annual International Conference of the IEEE Engineering in Medicine and Biology Society*, pages 4258–4261.

[Williams et al., 2002] Williams, G. N., Higgins, M. J., and Lewek, M. D. (2002). Aging skeletal muscle: Physiologic changes and the effects of training. *Physical Therapy*, 82(1):62–68.

[Yao et al., 2000] Yao, W., Fuglevand, R. J., and Enoka, R. M. (2000). Motor-unit synchronization increases emg amplitude and decreases force steadiness of simulated contractions. *J Neurophysiol*, 83(1):441–452.

[Zecca et al., 2002] Zecca, M., Micera, S., Carozza, M. C., and Dario, P. (2002). Control of multifunctional prosthetic hands by processing the electromyographic signal. *Critical Reviews in Biomedical Engineering*, 30(4-6):459–485.